Microwave-assisted synthesis of meso-carboxyalkyl-BODIPYs and an application to fluorescence imaging

Received 00th January 20xx,
Accepted 00th January 20xx

DOI: 10.1039/x0xx00000x

Neliswa Z.Mhlongo[a], Thomas Ebenhan[b,c], Cathryn H. S. Driver[b,d], Glenn. E. M. Maguire[a], Hendrick G. Kruger[a] and Thavendran Govender*[e] and Tricia Naicker*[a]

In this study, a significantly improved method for the synthesis of modular *meso*-BODIPY (boron dipyrromethene) derivatives possessing a free carboxylic acid group (which was subsequently coupled to peptides), is disclosed. This method provides a vastly efficient synthetic route with a > threefold higher overall yield than other reports. The resultant *meso*-BODIPY acid allowed for further easy incorporation into peptides. The *meso*-BODIPY peptides showed absorption maxima from 495-498 nm and emission maxima from 504-506 nm, molar absorptivity coefficients from 33383-80434 $M^{-1}cm^{-1}$ and fluorescent quantum yields from 0.508-0.849. The *meso*-BODIPY-c(RGDyK) peptide was evaluated for plasma stability and (proved to be durable even up to 4 h) was then assessed for its fluorescence imaging applicability *in vivo* and *ex-vivo*. The optical imaging *in vivo* was limited due to autofluorescence, however, the *ex-vivo* tissue analysis displayed BODIPY-c(RGDyK) internalization and cancer detection thereby making it a novel tumor-integrin associated fluorescent probe while displaying the lack of interference the dye has on the properties of this ligand to bind the receptor.

Introduction

Boron dipyrromethene (BODIPY)-based dyes (generally have absorption and emission peaks in the range of 480–540 nm) present remarkable spectroscopic properties such as narrow absorption bands, sharp emissions, high molar absorptivity coefficients and increased fluorescent quantum yields that can provide a high target to background ratio.[1] The majority of BODIPY dyes are; stable in the physiological pH-range, independent of solvent polarity with regards to its photophysical properties, and allow the study of deep-seeded tissue.[2] This class of dyes are also less susceptible to photochemical degradation[2-3] and are non-toxic to cells (when used as clinical probes the doses are substantially lower than the doses associated with toxicity).[1a, 4] Most recently these dyes have been coupled to photoremovable protecting groups expanding their use in cutting edge medical developments.[5] They have also proven to be ideal candidates for chemical modification at various positions of its core structure as illustrated in **Figure 1** allowing the tunability of its photophysical properties.[6]

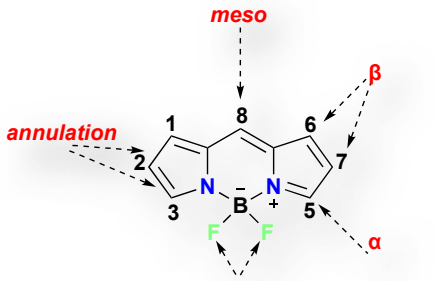

Figure 1: Basic molecular structure of the BODIPY dye.[6]

These suitable characteristics make these dyes excellent probes for use in biological systems and novel materials.[7] The total synthesis of the BODIPY dyes has usually suffered from low reaction yields and hence the largest drawback to the use of this type of core chemical structure.[1a, 8] Despite this challenge, these molecules have still managed to become a privileged class of organic dyes due to its real world applications across a wide range of research areas. Amongst the various synthetic routes to obtain these derivatives, one of the classic methods to the 8-substituted or *meso* BODIPY derivatives remains the condensation between acid anhydrides with pyrroles with overall reaction yields ranging from 5-25% (Scheme 1).[4a, 9] The resulting free carboxylic acid or active esters produced can be used as a handle to attach it to targeting molecules. Improved synthetic approaches for such BODIPY derivatives will allow for better synthetic accessibility and increased interest in its conjugation to receptor binding molecules.[9d, 10]

Herein, we report the most viable, convenient and economic method to date for the synthesis of the *meso*-BODIPY core with

[a] Catalysis and Peptide Research Unit, University of KwaZulu-Natal, Durban, South Africa
[b] Preclinical Imaging Facility, Nuclear Medicine Research Infrastructure, , Pretoria, South Africa
[c] Nuclear Medicine Department, University of Pretoria, Pretoria, South Africa.
[d] Radiochemistry, South African Nuclear Energy Corporation, Pretoria, South Africa
[e] Department of Chemistry, University of Zululand, Private Bag X1001, KwaDlangezwa 3886, South Africa
Email govendert@unizulu.ac.za or naickert1@ukzn.ac.za

a free carboxylic handle. Secondly, a proof-of-principle, including demonstration of serum stability and the fluorescence imaging applicability (*ex vivo* and *in vivo*) of the c(RGDyK) peptide derivative of this *meso*-BODIPY is reported for the first time.

Results and Discussion

Initially, the synthesis of the free acid *meso*-BODIPY derivative was attempted following the seminal report by Li *et al.*[9a] This method involves refluxing the starting materials, glutaric anhydride (**1**) and 2,4-dimethylpyrrole (**2**), in DCM with $BF_3.OEt_2$ for 5 hours, resulting in the formation of intermediate **3**. This was further reacted with excess $BF_3.OEt_2$ at room temperature overnight to yield the desired product **4** shown in **Scheme 1**. This procedure proved to be irreproducible in our hands even after several minor modifications which included; stricter moisture control, increased reaction times and elevated reaction temperatures. Analysis of the reaction mixtures via LC-MS revealed that only the starting material was present, and that no intermediate or product had formed.

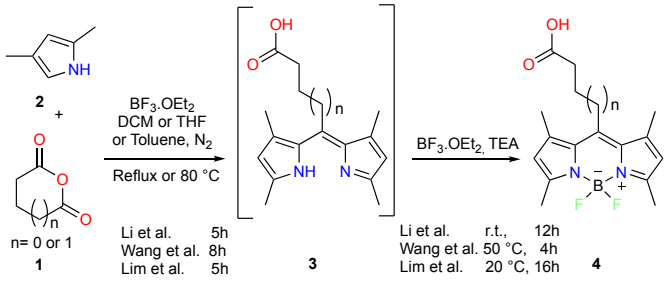

Scheme 1: Synthetic route towards obtaining BODIPY derived acid[4a, 9a, b]

The method reported by Wang *et al.,* which employs THF as the solvent, was subsequently attempted.[9b] This approach formed intermediate **3** albeit in less than 5% yields (as judged by LC-MS analysis) after 48 hours (reflux) with starting materials still present as the major constituents. Despite carrying out experiments using extended reaction times and elevated temperatures, no significant increases in the formation of the intermediate **3** were observed.

Next, the longer synthetic route reported by Pakhomov *et al.,* which involved the opening of the cyclic acid anhydride (**5**) ring before its condensation with 2,4-dimethylpyrrole was also attempted (**Scheme 2**).[11]

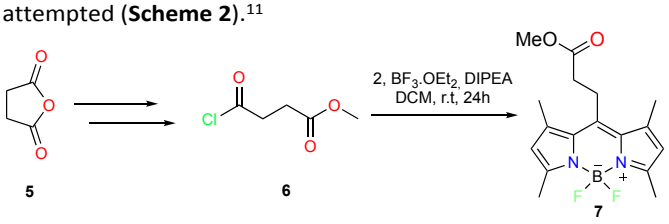

Scheme 2: Synthetic route towards obtaining BODIPY derived ester[11]

Although the formation of **6** was successful, the yield of the methyl ester intermediate **7** (reported to be 36 %), in our case was <10 % since the reaction of **6** with **2** did not proceed to any further (**7** was not isolated). Thereafter, we decided to revisit the one pot method since this seemed to give better conversion of starting materials. Lim *et al.*[4a] reported a method whereby they used toluene as the solvent and succinic anhydride (**5**) to get the product in 18% yield after 21 hours. In our hands, we could not see any significant formation of the corresponding intermediate **3** when using succinic anhydride but did get conversion with glutaric anhydride (< 20 % conversion; 48 h).

Upon complexation with $BF_3.OEt_2$, only approximately 7 % of the product **4** formed after 3 days at room temperature. Despite the low yields and longer reaction times, the acquisition of the product after the first 3 attempts deemed this method promising for further optimization. Microwave irradiation (15 min, 80 ^{o}C) of glutaric anhydride (**1**) with pyrrole (**2**) and $BF_3.OEt_2$ in toluene led to the consumption of all of the starting material. As expected from microwave based reactions, it was faster than previous attempts with conventional heating, reproducible, fewer by-products and increased yields of **4** (56 %) (**Scheme 3**). The presence of starting materials was observed for shorter reaction times or lower temperatures for the microwave step. Whilst, shorter reaction times at higher temperature resulted in many by-products.

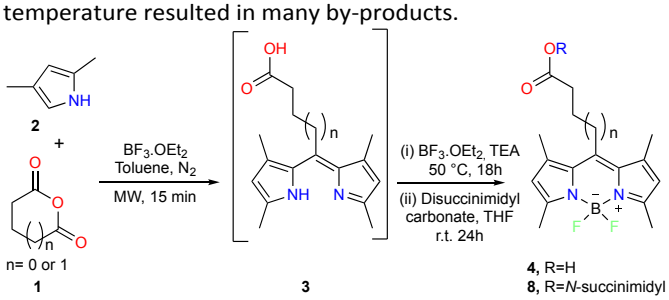

Scheme 3: Synthetic route towards obtaining BODIPY derived acid or ester

Specific reaction conditions i.e. the molar equivalents of starting reagents 2,4-dimethylpyrrole (7 eq.) and $BF_3.OEt_2$ (3 eq.) were optimised for reaction completion in 15 min as this subsequently influenced the improved yield of the final product **4**. While microwave irradiation has been reported in the derivatization of BODIPY,[12] to the best of our knowledge this is the first report where this heating method has been employed in the synthesis of the core structure.

Although the dipyrromethene intermediate **3** has been reported to be stable, easy to handle and/or to purify,[1a] it was not isolated during this synthesis. In our case, the LC-MS trace showed complete conversion of the limiting reagent (glutaric anhydride) and the resultant intermediate **3**, presenting as a brick red solution that was subsequently carried through to the next step (**Scheme 3**).[4a] Initial investigation of the conversion from intermediate **3** to product **4** using excess $BF_3.OEt_2$ and triethylamine at room temperature (as per Li *et al.* and Lim *et al.),* did not give yields > 15 %, even upon extended reaction times (1-24 hours). The optimal temperature was found to be 50 ^{o}C (as per Wang *et al.*), where the product formed in 18 hours with minimal amounts of the intermediate remaining and no side product formation. Longer reaction times did not have any significant influence on the reaction yields (**Scheme 3**). After optimization, the reaction was quenched with 0.1 M HCl and purified *via* silica gel column chromatography to furnish compound **4** as red crystals. The reaction was scaled up from 50 mg to 500 mg and showed improved yields (56 and 65 % respectively) as compared to previous reports for

this *meso*-carboxyalkyl BODIPY derivative which ranged from 5-25 %.[4a, 9] The improvement in the synthesis of this dye is a significant breakthrough in the production of a compound that is well known to suffer from low reaction yields.[1a] The structure of compound **4** was confirmed by NMR spectroscopy, LC-MS, HRMS and X-ray crystallography (CCDC code 1962482). The proton and carbon NMR spectral data resembled that was previously reported in literature.[9a] Next, the succinic anhydride reaction was revisited by applying our optimised conditions. The intermediate formed smoothly after 15 minutes in the microwave and the subsequent condensation proceeded well with none of the intermediate remaining (monitored by LC-MS). After workup, the reaction mixture was purified *via* silica gel column chromatography to furnish the analogous acid **4** as a dark red powder (60 % yield). The proton and carbon NMR spectral data resembled that was previously reported in literature.[9b] This proved the generality of our microwave assisted method for the synthesis of meso-substituted BODIPY dyes. The advantages of this synthetic approach are that it is short, high yielding, and a one-pot-reaction, thereby making it more convenient as compared to reported methods. Attractively, the product produced contains a free carboxylic acid which can further be easily attached to target molecules.[1a] Moreover, the *meso*-substituted BODIPY derivative has a rigid structure that is modular, making it an attractive target for peptide/polymer conjugation.[13]

In pursuit of BODIPY-peptides for *in vivo* applications, compound **4** was subsequently converted into its *N*-hydroxy succinimide (NHS) activated ester **8** for easy couplings with peptide amino groups and to improve the slow reaction kinetics of free carboxylic acids.[14] Activated esters, particularly that of *N*-hydroxy succinimide have good reactivity and selectivity for amino groups as it is susceptible to nucleophilic attack by primary amines.[14] This feature allows for conjugation to a variety of antibodies, peptides and proteins to form fluorescent tracers for cellular labelling and detection. The synthesised derivative **8** has a C_4-alkyl spacer between the fluorophore and the NHS ester group. This spatial separation between the fluorophore and its point of attachment to the biomolecule is a common structural alteration that helps to minimize the interaction of the sometimes-bulky fluorophore with the biomolecule to which it is conjugated. Despite, *N*-hydroxy succinimide being a common reagent for the activation and coupling of carboxylic acids, in this study, *N, N'*-disuccinimidyl carbonate proved to be a superior coupling reagent[15] for the formation of **8** (**Scheme 3**). The reaction was conducted according to a previously reported method[9b] to yield compound **8** as an orange powder in 99 % yield. The synthesis was performed in a one-pot reaction without the requirement of chromatographic purification. The proton NMR data resembled that reported in literature.[9b]

The completion of the synthesis of a BODIPY-conjugate required coupling of the activated BODIPY-ester to a peptide. Towards this end, the BODIPY-succinimidyl ester **8** was firstly coupled to a small, commercially available peptide, β-Ala-tripeptide, supported on chlorotrityl chloride (CTC) resin to afford peptide **9** (**Figure 3**). This system was chosen for its convenience as a supported peptide to evaluate the coupling efficiency to the activated BODIPY ester. The peptide coupling was achieved through the conjugation of the BODIPY-succinimidyl ester with the ϵ-amino group of the alanine residue. Upon cleavage from the resin, the LC-MS trace showed complete conversion of all starting materials and the novel product **9** was obtained as an orange powder in quantitative yields. The product and purity was confirmed with HRMS and LC-MS analysis.

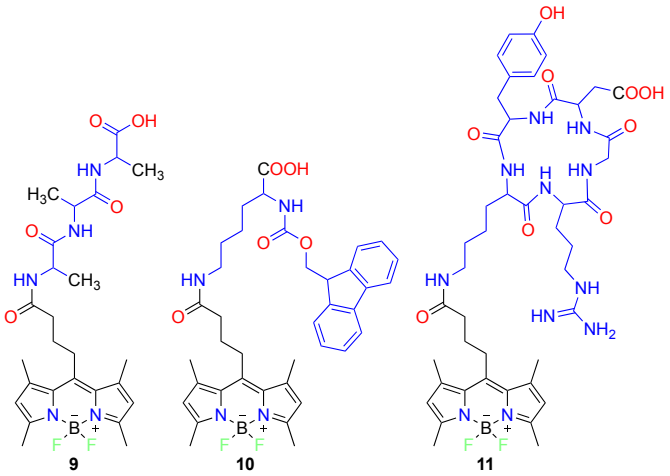

Figure 3: BODIPY derived peptides that were synthesised from activated ester **8**.

For further evaluation, the BODIPY succinimidyl ester **8**, was coupled to an unsupported, protected amino acid, Fmoc-Lys(4-methoxytrityl)-OH. The novel Fmoc-Lys (BODIPY) derivative **10** was synthesized by coupling of **8** to the lysine amino group of Fmoc-Lys(Mmt)-OH **(Figure 3)**. The Mmt group was deprotected before it's coupling to the ester. This reaction was purified using supercritical fluid chromatography (SFC) to give compound **10** as an orange powder in 66% yield. The product was confirmed with LC-MS (*m/z* 683 $[M-H]^-$) after purification with SFC. Generally, BODIPY dyes are purified using column chromatography (either flash/gravity) or preparative HPLC.[16] Here, we report to the best of our knowledge for the first time, the purification of a BODIPY compound using SFC. The SFC purification provides high purity compounds in a shorter analysis time and is easy to operate. Moreover, the method is greener, faster and less expensive compared to typical HPLC.[17]

Finally, the experience of the initial coupling reactions allowed for **8** to be coupled to a biologically relevant peptide, cyclic(RGDyK). The *meso*-BODIPY-c(RGDyK) (**11**) was achieved through the conjugation of BODIPY-succinimidyl ester with the ϵ-amino group of the lysine residue by adapting the literature method,[18] (**Figure 3**). Interestingly, the base we employed in this reaction was polymer bound triethylamine (diethylaminomethyl polystyrene resin) that made purification much easier. The desired product was isolated from the reaction mixture and the polymer resin with 5 % acetonitrile in water using a centrifuge. The combined supernatant washings were freeze-dried to give compound **11** as an orange powder with 90 % yield. The reaction was monitored with LC-MS analysis of the product peak (*m/z* 936 $[M+H]^+$) and further characterization was done by HRMS with the purity confirmed by HPLC analysis. While different derivatives of BODIPY-RGD peptides have been reported,[18] the synthesis of compound **11** has not been previously reported.

The absorption and the emission properties of fluorescent dyes are very important in bioanalysis such as fluorescence imaging. The absorption and the emission spectra of the synthesized *meso*- carboxyalkyl BODIPY dye (**4**), *meso*-BODIPY-NHS (**5**) and

meso-BODIPY peptides (**9-11**) displayed typical characteristics of BODIPY dyes with the absorption and the emission maxima around ~500 nm and ~ 510 nm, respectively, in ethanol (**Suppl**, **Table 1**) . No significant shifts in absorbance and emission wavelengths were observed with the addition of peptide substituents to the *meso*-carboxyalkyl BODIPY derivative. This phenomenon is attributed to the *meso*-functionalised position of the derivatives which ensures that the BODIPY core is electronically isolated from the substituents and therefore remains unaffected.[1a] The compounds showed a strong electron transition in the visible region with molar absorptivity coefficients ranging from 3716.3 $M^{-1}.cm^{-1}$ to 80434 $M^{-1}.cm^{-1}$. The fluorescence quantum yield of the synthesized dyes were determined in ethanol with the standard fluorescein in 0.1 M NaOH as a reference compound. BODIPY derivatives bearing the free carboxylic acid at the *meso*-position showed the higher fluorescent quantum yields (0.849) than the peptide derivatives which were **9** (0.609), **10** (0.525) and **11** (0.508). The spectroscopic characterisation results for the *meso*-carboxyalkyl BODIPY (**4**) were similar to that previously reported in ethanol.[5b, 9b] The remaining compounds **9-11** were novel and their spectroscopic properties were determined using the reported procedure as that for compound **4**.[9b]

Serum Stability

The majority of BODIPY dyes are known to be relatively insensitive to the changes in the environment with regards to its photochemical stability.[1b, 3c, 19] However, peptides can undergo enzymatic degradation in biological fluids.[20] In order to evaluate the BODIPY-c(RGDyK) as a preclinical optical imaging agent, its intravenous administration was considered to be the desired route of injection; hence, determining the stability of this conjugate in serum was essential before the *in vivo* evaluation. **Figure 4** shows the LC-MS chromatograms of a serum sample spiked with BODIPY-RGD peptide (1.0 µg/mL). The serum stability study was performed following the method that was previously reported in our group.[21] The LC-MS-ESI was used to monitor the recoveries and the peptide was shown to be stable throughout the analysis period (4 hours). These results were similar to that previously reported on the serum/plasma stability test of other BODIDIPY-RGD peptides[22].

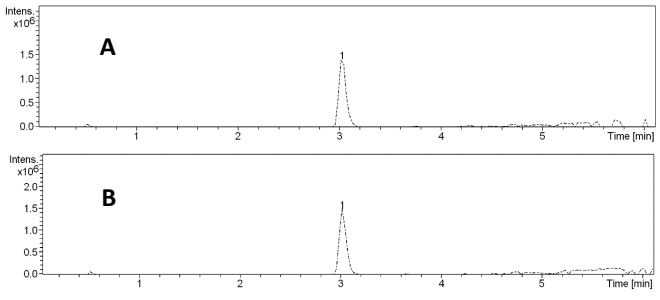

Figure 4: HPLC chromatogram of serum that is spiked with BODIPY-c(RGDyK) peptide: **A** at 0 h and **B** at 4h.

BODIPY-c(RGDyK) Fluorescence Imaging *in vivo*

The prospects of using novel BODIPY-peptide conjugates for non-invasive tumour detection or non oncological application are encouraging as their design would potentially allow for combined used nuclear-optical imaging modalities in future.[18, 23] Therefore, after full characterization of the BODIPY-peptide derivatives, BODIPY-c(RGDyK) **11** was further assessed for its fluorescence imaging usefulness (*in vivo* and *ex vivo*) in healthy and MCF-7 tumour-bearing female nude mice. Optical fluorescence imaging has the advantage over other diagnostic methods as one can study tumour proliferation and changes in tumour response to therapy non-invasively, often supporting a better understanding of disease progression.[24] The BODIPY-c(RGDyK) fluorescence imaging efficacy was evaluated using MCF-7 breast cancer xenografts as previous studies highlighted high αvβ3 integrin expression in these tumour cells[25] and which was confirmed *in vivo* by RGD-based ligands.[26] Athymic nude animals are desired for optical imaging since firstly, the hairless condition allows for a more accurate visualisation, quantification and interpretation of the fluorescence imaging signal and secondly, the athymic condition allows tumour cell inoculation to grow out to relatively viable tumours as the immune system is not equipped to respond to the tumour cell invasion due to the depletion of T-helper cells.[27]

Prior to the animal investigation, a BODIPY-c(RGDyK) solution (containing 0.25 % DMSO) was assessed for its signal intensity using the optical camera equipment (**Suppl. Fig 5**) and combinations of available excitation (ex) and emission (em) filters in order to find the optimal filter pair (**Suppl. Fig 6**) to yield high overall counts. The maximum (peak) fluorescence (~50000 counts) was determined at wavelengths for λ_{ex} 480 nm/ λ_{em} 570 nm and λ_{ex} 520 nm/ λ_{em} 570 nm. The ex-filter with the lowest available wavelength of 420 nm showed markedly reduced peak fluorescence (~24500 counts) using an em-filter ≥ 520 nm. Signal intensity was negligible using wavelengths for λ_{ex} > 540 nm and λ_{em} >710 nm. These results are plausible as the λ_{max}(abs) for *meso*-BODIPY dye is 495 nm. Low fluorescence (<13500counts) was determined using em-filters ≥ 670 nm wavelength paired with all relevant ex-filters (420-540 nm) which restricts this *meso*-BODIPY moiety from an optimal imaging performance in the most desired near-infrared (> 750 nm) excitation and emission wavelengths.[2] The *meso*-BODIPY *in vivo* imaging technique at this stage may not be straightforward and its acquisition protocol would require extensive autofluorescence (AF) removal. AF is mostly tissue-generated (i.e. red blood cells and skin-based collagen; λ_{max} 400 – 600 nm) or occurs due to chlorophyll-containing food (λ_{ex} 680 nm). Even for bright optical markers, such as BODIPY, AF may not be fully eradicated and often prevents the detection of low intensity signals in the visible range. In preparation for this study, the animals were fed an alfalfa-free diet (low in chlorophyll) which would be beneficial to lower the diet related AF signal; however, a more promising technical solution for prospective studies may be the use of narrow bandpass emission filters combined with multispectral unmixing or the more straightforward continuation with a *meso*-BODIPY derivative that can be excited at wavelengths in the near-infrared that is less prone to interferences with AF.[28]

The fluorophore formulation was individually diluted for each animal and prepared in 0.25 mL and deemed suitable for a first injection (DMSO/dose: 0.62 ± 0.42 % (equ in blood: 0.046 ± 0.031 %)) administering a 0.15 mL bolus via the tail vein (injected doses ranged from 25-167 pmol/g bodyweight). In all animals (n = 5) BODIPY-c(RGDyK) injections did not cause any adverse reactions and no significant changes in mice bodyweights were measured (19.4 ± 1.3 and 18.6 ± 1.7; $P < 0.05$) between the start and termination of the experiment, respectively. Between 5 and 20 % of the injected dose was recognized in the area of the tail as seen from unspecifically localized fluorescence signal. This is likely due to non-quantitative injections or probe leakages sometimes occurring into the interstitial tissues surrounding the tail vein.

Despite the expected limitation regarding AF removal, real-time whole-body imaging was performed at 3 h and 24 h for a general understanding of the probe's behaviour in living organisms. **Figure 5A** shows a background-corrected image of a representative mouse with a sustained fluorescence signal when comparing the earlier and late time point of imaging. Tumor bearing animals demonstrated no significant BODIPY-c(RGDyK) signal in the tumor area (see arrow in **Figure 5B**) which is plausible as the properties of the *meso*-BODIPY-moiety may be technically challenged for *in vivo* application; however, these animals were also subjected to *ex vivo* analysis of organ and tissue uptake of BODIPY-c(RGDyK) (**Figure 5C**).

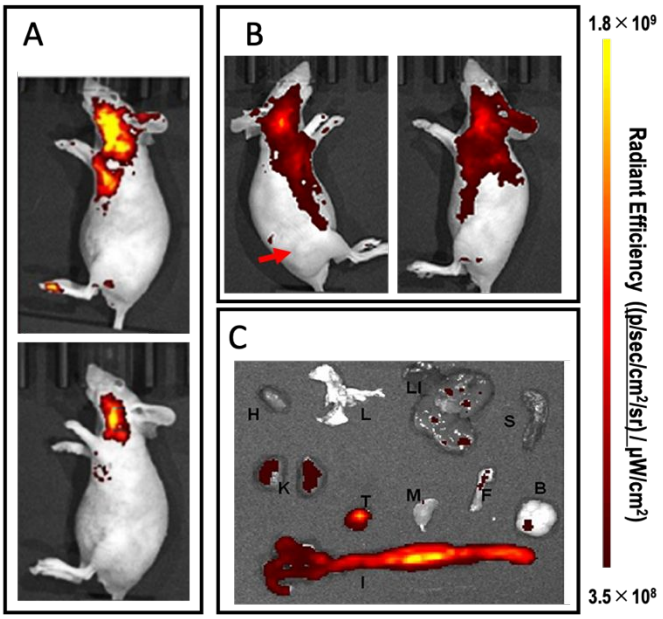

Figure 5: Overview of BODIPY-c(RGDyK) Fluorescence Imaging. **A** Representative images of a nu/nu balb/c mouse showing BODIPY-c(RGDyK) fluorescence signal (radiant efficiency)*in vivo* at 3 h (top) and 24 h (bottom)following intravenous probe injection; image exposure time(sec) /binning/ f-stop = 0.5/ 8/ 2.0.**B** *In vivo* tumour visualization of a representative nude balb/c mouse bearing a MCF-7 tumor xenograft (red arrow indicates tumor location) in the hind flank (left image) compared to the contralateral side (without tumor; right image); image exposure time(sec) /binning/ f-stop = 0.5/ 8/ 2.0. **C** Qualitative *ex vivo* organ and tissue analysis; representative biodistribution at 24 h after administration (image exposure time (sec)/ binning/ f-stop = 2.0/ 8/2.0). Displayed organ/tissues are: H= heart, L=lung, LI=liver, S=spleen, K=kidneys, T-=tumour, M=muscle, F= femur (bone), B=brain and I= intestines.

Ex vivo biodistribution has the benefit of clearly providing information of organ involvement in the metabolism of novel optical probes, without the quenching of specific signal due to the AF processes; reference tissue can therefore directly be compared with pathological tissue such as the MCF-7 tumours dissected in this study. The bright light organ images with their fluorescence signal overlays for this study are displayed in **Figure 5C**. Whilst *in vivo* imaging could not visualize the tumors, *ex vivo* analysis of organ-related fluorescence at 24 h post BODIPY-c(RGDyK) injection showed an intense signal in the tumor and also in intestines with some notable signal deriving from the kidneys. This may indicate that this probe was *i*) completely eliminated from the blood pool (no notable heart fluorescence signal), *ii*) was predominantly excreted (renal and intestinal) and *iii*) a plausible signal observed for MCF-7 tumours may be αvβ3 integrin-mediated and therefore considered a targeted tumor cell accumulation (i.e. BODIPY-c(RGDyK) was capable of penetrating into the tumor tissue). Further investigations may be required to confirm specific tumour uptake of BODIPY-c(RGDyK); however, these first findings are in agreement with *ex vivo* optical imaging and confocal microscopy imaging performed in other investigations with RGD-based imaging probes.[25-26] These results may necessitate that a bioconjugate of a *meso*-BODIPY moiety with c(RGDyK) be further developed to support *ex vivo* analysis of organ biodistribution and for investigation of different cancers via targeting of αvβ3 integrin which can be overexpressed during tumour angiogenesis.

Conclusions

This study significantly improved the synthetic route of the core *meso*-carboxyalkyl BODIPY derivative which was successfully converted into its activated ester to further yield three novel BODIPY-peptide conjugates. The carboxyalkyl BODIPY derivative (**4**, n=0,1) was synthesized for the first time using a microwave assisted method. Furthermore, the BODIPY peptide (**10**) was successfully purified for the first time using supercritical fluid chromatography technology thereby providing an innovative alternative for the isolation of BODIPY dyes. The synthesized derivatives displayed typical spectroscopic characteristics of BODIPY dyes while the BODIPY-c(RGDyK) peptide (**11**) proved to be stable in plasma. Approaching the fluorescent imaging performance of BODIPY-c(RGDyK) for its *ex vivo* imaging application, the αvβ3 integrin-mediated targeting process in MCF-7 breast cancer xenografts was envisaged as a proof-of-principle investigation. Despite the interference of the *in vivo* analysis by autofluorescence, the *ex vivo* results showed that the fluorophore does undergo cellular internalization and this may have implications for cancer detection. The *in vivo* optical imaging with the fluorophores developed in this study can be enhanced by further derivatizing the modular acid (**4**) to shift its absorption and emission maxima from the green to the near-infrared region of the electromagnetic spectrum. Additionally, the fluorophores can

also be used for other *in vitro* applications such as fluorescent assays or microscopy.

Conflicts of interest

There are no conflicts to declare.

(Z)-3-(3,5-dimethyl-1H-pyrrol-2-yl)-3-(3,5-dimethyl-2H-pyrrol-2-ylidene) propanoic acid (3)[4a]

To an overdried 40 mL microwave tube, glutaric anhydride or succinic anhydride (500 mg, 1.0 eq.), dry toluene (3.0 mL), 2,4-dimethylpyrrole (3.1 mL, 7.0 eq.) and $BF_3.OEt_2$ (1.6 mL, 3.0 eq.) were added consecutively under a nitrogen atmosphere. The mixture was heated with high stirring for 15 minutes at 80 °C in the microwave at 200 watts to yield compound **3** as a brick-red solution. The reaction was monitored with LC-MS until consumption of the limiting starting material. The product was used as is for the next step without further purification and or isolation.

4-(4,4-Difluoro-1,3,5,7-tetramethyl-4-bora-3a,4a-diaza-s-indacene-8-yl)-butyric acid (4)[4a]

To the reaction mixture of compound **3,** dry triethylamine (4.88 mL, 10.0 eq.) was added, after 15 minutes, $BF_3.OEt_2$ (12.43 mL, 20.0 eq.) was added dropwise at room temperature under a nitrogen atmosphere. The reaction mixture was then stirred with heating at 50 °C for 18 hours (under nitrogen). Thereafter, ethyl acetate (20 mL) was added and the mixture was washed with 0.1 M HCL (3 x 10.0 mL). After the liquid-liquid extraction, the organic phase was dried with anhydrous $NaSO_4$ and the solvent was evaporated *in vacuo*. The resulting residue was purified by column chromatography (0-30 % ethyl acetate in hexane) to provide compound **4** (glutaric) as brick red needle-like powder, Rf = 0.29, (50:50 hexane:ethyl acetate), mass 962.01 mg; yield 65.6 %; LC-MS *m/z* = 333 [M-H]$^-$, ^{1}H NMR δ 6.05 (s, 2H), 3.05 – 3.01 (t, 2H, J = 8.8 Hz), 2.56 -2.51 (t, 2H, J = 8.8 Hz), 2.51 (s, 6H), 2.42 (s,6H), 1.99 – 1.95 (m, 2H); ^{13}C NMR δ 176.9, 154.3, 144.7, 140.37, 131.4, 121.8, 33.7, 27.3, 26.5, 16.3, 14,4; ^{19}F NMR δ 146.3 – 146.7. HRMS (ESI) *m/z* calculated for $C_{17}H_{21}BF_2N_2O_2$ 334.1718, found *m/z* 334.1718

4-(4,4-Difluoro-1,3,5,7-tetramethyl-4-bora-3a,4a-diaza-s-indacene-8-yl)-butyric succinimidyl ester (8)[9b]

To a 15.0 mL oven-dried pear shape flask, compound **4** (250.0 mg, 1.0 eq.), *N*, *N*'-disuccinimidyl carbonate (383.0 mg, 2.0 eq.), dry THF (4.0 mL) and dry TEA (0.75mL) were added consecutively under a nitrogen atmosphere. After stirring for 20 hours at room temperature, the reaction was monitored with LC-MS for consumption of all starting material. The THF was removed *in vacuo* and the resulted orange powder was dissolved in DCM (10.0 mL) and washed with saturated sodium hydrogen carbonate (4 × 10.0 mL). The organic phase was dried with anhydrous $NaSO_4$ and the solvent was evaporated *in vacuo* to give compound **8** as an orange powder. Mass 673.10 mg, yield 99.9%, LC-MS *m/z* 432 [M + H]$^+$, ^{1}H NMR δ 6.06 (s, 2H), 3.12-3.087(t, 2H, J = 8.8 Hz), 2.85 (s, 4H), 2.82 – 2.78 (t, 2H, J = 8.8 Hz), 2.51 (s, 6H), 2.42 (s, 6H), 2.08 -2.04 (m, 2H); ^{13}C NMR δ 168.9, 167.8, 154.4, 143.9, 140.4, 131.4, 121.9, 30.9, 27.0, 26.2, 25.6, 14.4, 14.5; ^{19}F NMR δ -146.4 – 146.6, HRMS (ESI) m/z calculated for $C_{21}H_{24}BF_2N_3NaO_4$ 454.1720, found *m/z* 454.1714.

4-(4,4-Difluoro-1,3,5,7-tetramethyl-4-bora-3a,4a-diaza-s-indacene-8-yl)-butyricamide-Ala-tripeptide (9)

The peptide synthesis was carried out manually in a 5.0 mL plastic syringe fitted with a Whatman filter paper disc and a stopper at the bottom. Ala-tripeptide-CTC (439.5 mg, 1.0 eq.) was added and washed with DCM (2 x 2.0 mL) over 20.0 min placed in a shaker. Thereafter, compound **8** (94.7 mg, 2.0 eq.) dissolved in DMF (2.0 mL) and DIPEA (100.0 µL, 5.0 eq.) were added to the peptide on the shaker. The mixture was left shaking at room temperature for 1.5 hour and thereafter the DMF was drained. Compound **9** bound on the resin was washed with ether (2 × 10 mL). To cleave the resin 1% TFA in DCM was used and the resin was filtered off through a plug of cotton wool to achieve compound **9** as orange powder once the DCM was evaporated. The reaction was monitored with LC-MS which confirmed the consumption of all starting materials. LC-MS *m/z* 546 [M-H]$^-$, HRMS (ESI) *m/z* calculated for $C_{26}H_{36}BF_2N_5NaO_5$ 570.2670, found *m/z* 570.2674.

Fmoc-Lys(4-(4,4-Difluoro-1,3,5,7-tetramethyl-4-bora-3a,4a-diaza-s-indacene-8-yl)butyricamide) peptide (10)

To a 15.0 mL falcon centrifuge tube, Fmoc-Lys (Mmt)-OH (100.0 mg, 1.0 eq.) was dissolved in 1.0 % TFA in DCM and stirred for approximately 1.0 h at room temperature to remove the Mmt protection. The TFA was evaporated with a stream of nitrogen, thereafter, compound **5** (117.11 mg, 1.0 eq.) and diethylaminomethyl-polystyrene (424.4 mg, 5.0 eq.) in DMF 4.0 mL were added to the tube. The reaction mixture was placed on the shaker for 2.0 hours at room temperature. The LC-MS of the crude mixture confirmed the product with *m/z* 683 [M-H]$^-$ with consumption of the starting material. Then the reaction was centrifuged for 10.0 min in 200.0 rpm at 4 °C. The supernatant was decanted and DMF (2.0 mL) was added, the reaction was centrifuged again. This step was repeated until all the no more product appeared in the DMF layer. All the washings were then combined and the DMF sublimed using the freeze dryer to give a dark orange sticky paste. The crude product was purified using a Sepiatec SFC system in isocratic separation mode with a Supelco-GreenSep™ Nitro SFC column (25 cm ×4.6 mm × 5 µm) and 10:90 modifier (acetonitrile): supercritical-CO_2 with the flow rate of 6.0 mL/min for 6.0 min . The collection from the SFC was evaporated *in vacuo* to yield compound **10**. Mass 123.3 mg. Yield 66.3%. HRMS (ESI) *m/z* calculated for $C_{38}H_{43}BF_2N_4NaO_5$ 707.3210, found *m/z* 707.3187.

4-(4,4-Difluoro-1,3,5,7-tetramethyl-4-bora-3a,4a-diaza-s-indacene-8-yl)-butyricamide cyclic RGD peptide (11)[18]

To a dry 1.5 mL microcentrifuge eppendorf tube, the cyclic RGD peptide (5.0 mg, 1.0 eq.), compound **8** (2.9 mg, 1.0 eq.), diethylaminomethyl-polystyrene (61.4 mg 1.0 eq.) and dry DMSO (307.1 µL) were added consecutively. The mixture was placed on the shaker at room temperature and the reaction was monitored with LC-MS until all consumption of the starting material. After 24 hours, millipore water (200 µL) was added to the mixture and it was placed under the freeze-drier overnight to remove the DMSO and water to give an orange powder. This step was repeated to ensure that all the solvent was removed. Thereafter, the product was extracted using the centrifuge by adding 1 mL of 5% acetonitrile in water and the supernatant was decanted (this was repeated until no product was seen (in supernatant) from LC-MS monitoring), thereafter all the washings were combined and freeze-dried to give compound **11** as orange powder, mass 6.8 mg, yield 90.7 %. The product and purity was confirmed with LC-MS *m/z* 936 $[M+H]^+$, HRMS (ESI) *m/z* calculated for $C_{46}H_{64}BF_2N_{12}O_9$ 777.89, found 977.845.

Acknowledgements

The authors would like to thank the South African National Research Foundation, the Nuclear Medicine Research Infrastructure, and the Medical Research Council for the financial support.

Notes and references

‡ All spectra and further experimental procedures are provided as supplementary information.

1. (a) A. Loudet and K. Burgess, *Chem. Rev.*, 2007, **107**, 4891-4932; (b) G. Ulrich, R. Ziessel and A. Harriman, *Angew. Chem., Int. Ed.*, 2008, **47**, 1184-1201.
2. D. Shcherbo, E. M. Merzlyak, T. V. Chepurnykh, A. F. Fradkov, G. V. Ermakova, E. A. Solovieva, K. A. Lukyanov, E. A. Bogdanova, A. G. Zaraisky, S. Lukyanov and D. M. Chudakov, *Nature Nat. Med.*, 2007, **4**, 741-746.
3. (a) E. Ozcan, G. Kesan, B. Topaloglu, E. Tanriverdi Ecik, A. Dere, F. Yakuphanoglu and B. Cosut, *New J. Chem.*, 2018, **42**, 4972-4980; (b) S. Zhang, T. Wu, J. Fan, Z. Li, N. Jiang, J. Wang, B. Dou, S. Sun, F. Song and X. Peng, *Org. Biomol. Chem.*, 2013, **11**, 555-558; (c) B. Hinkeldey, A. Schmitt and G. Jung, *ChemPhysChem*, 2008, **9**, 2019-2027.
4. (a) S. H. Lim, C. Thivierge, P. Nowak-Sliwinska, J. Y. Han, H. van den Bergh, G. Wagnieres, K. Burgess and H. B. Lee, *J. Med. Chem.*, 2010, **53**, 2865-2874; (b) M. Laine, N. A. Barbosa, A. Kochel, B. Osiecka, G. Szewczyk, T. Sarna, P. Ziolkowski, R. Wieczorek and A. Filarowski, *Sens. Actuators B Chem.*, 2017, **238**, 548-555; (c) R. Alford, H. M. Simpson, J. Duberman, G. C. Hill, M. Ogawa, C. Regino, H. Kobayashi and P. L. Choyke, *Mol. Imaging*, 2009, **8**, 341-354.
5. (a) K. Sitkowska, M. F. Hoes, M. M. Lerch, L. N. Lameijer, P. van der Meer, W. Szymański and B. L. Feringa, *Chem. Comm.*, 2020, **56**, 5480-5483; (b) J. L. Donnelly, D. Offenbartl-Stiegert, J. M. Marín-Beloqui, L. Rizzello, G. Battaglia, T. M. Clarke, S. Howorka and J. D. Wilden, *Chem. Eur. J.*, 2020, **26**, 863-872.
6. Rebeca Sola Llano, Edurne Avellanal Zaballa, Jorge Bañuelos, César Fernando Azael Gómez Durán, José Luis Belmonte Vázquez, E. P. Cabrera and I. L. Arbeloa, in *Photochemistry and Photophysics - Fundamentals to Applications*, eds. S. Saha and S. Mondal, IntechOpen, 2018, DOI: 10.5772/intechopen.74848, ch. Two.
7. (a) M. Gao, F. Yu, C. Lv, J. Choo and L. Chen, *Chem. Soc. Rev.*, 2017, **46**, 2237-2271; (b) A. Bessette and G. S. Hanan, *Chem. Soc. Rev.*, 2014, **43**, 3342-3405.
8. (a) R. Ziessel, G. Ulrich and A. Harriman, *New J. Chem.*, 2007, **31**, 496-501; (b) G. Ulrich, R. Ziessel and A. Harriman, *Angew. Chem., Int. Ed.*, 2008, **47**, 1184-1201.
9. (a) Z. G. Li, E. Mintzer and R. Bittman, *J. Org. Chem.*, 2006, **71**, 1718-1721; (b) D. C. Wang, J. L. Fan, X. Q. Gao, B. S. Wang, S. G. Sun and X. J. Peng, *J. Org. Chem.*, 2009, **74**, 7675-7683; (c) M. Collot, E. Boutant, M. Lehmann and A. S. Klymchenko, *Bioconjugate Chem.*, 2019, **30**, 192-199; (d) C. Ji, Y. Liang, F. Ge, L. Yang and Q. Wang, *Anal. Chem.*, 2019, **91**, 7032-7038.
10. (a) A. Haque, M. S. H. Faizi, J. A. Rather and M. S. Khan, *Bioorg. Med. Chem.*, 2017, **25**, 2017-2034; (b) Y. Ha and H. K. Choi, *Chem Biol Interact*, 2016, **248**, 36-51.
11. A. A. Pakhomov, Y. N. Kononevich, M. V. Stukalova, E. A. Svidchenko, N. M. Surin, G. V. Cherkaev, O. I. Shchegolikhina, V. I. Martynov and A. M. Muzafarov, *Tetrahedron Lett.*, 2016, **57**, 979-982.
12. (a) R. S. Yalagala, S. A. Mazinani, L. A. Maddalena, J. A. Stuart, F. Y. Yan and H. B. Yan, *Carbohydr. Res.*, 2016, **424**, 15-20; (b) T. Rohand, W. W. Qin, N. Boens and W. Dehaen, *Eur. J. Org. Chem.*, 2006, DOI: 10.1002/ejoc.200600531, 4658-4663; (c) J. H. Gibbs, Z. Zhou, D. Kessel, F. R. Fronczek, S. Pakhomova and M. G. H. Vicente, *J. Photochem. Photobiol., B*, 2015, **145**, 35-47; (d) F. Heisig, S. Gollos, S. J. Freudenthal, A. El-Tayeb, J. Iqbal and C. E. Muller, *J. Fluoresc.*, 2014, **24**, 213-230.
13. T. Nabeshima, M. Yamamura, G. J. Richards and T. Nakamura, *Yuki Gosei Kagaku Kyokaishi*, 2015, **73**, 1111-1119.
14. E. Valeur and M. Bradley, *Chem. Soc. Rev.*, 2009, **38**, 606-631.
15. H. Ogura, T. Kobayashi, K. Shimizu, K. Kawabe and K. Takeda, *Tetrahedron Lett.*, 1979, **20**, 4745-4746.
16. (a) E. Caruso, M. Gariboldi, A. Sangion, P. Gramatica and S. Banfi, *J. Photochem. Photobiol., B*, 2017, **167**, 269-281; (b) S. Dixit, T. Mahaddalkar, M. Lopus and N. Agarwal, *J. Photochem. Photobiol., A*, 2018, **353**, 368-375; (c) S. Krajcovicova, J. Stankova, P. Dzubak, M. Hajduch, M. Soural and M. Urban, *Chem. Eur. J.*, 2018, **24**, 4957-4966.
17. K. Govender, T. Naicker, S. Baijnath, A. Amichund Chuturgoon, N. Sheik Abdul, T. Docrat, H. Gerhardus Kruger and T. Govender, *J. Chromatogr., B*, 2020, DOI: https://doi.org/10.1016/j.jchromb.2020.122126, 122126.
18. (a) M. Ono, H. Watanabe, Y. Ikehata, N. Ding, M. Yoshimura, K. Sano and H. Saji, *Sci. Rep.*, 2017, **7**, 1-11; (b) S. Liu, T. P. Lin, D. Li, L. Leamer, H. Shan, Z. Li, F. P. Gabbai and P. S. Conti, *Theranostics*, 2013, **3**, 181-189.

19. (a) A. Kamkaew, S. H. Lim, H. B. Lee, L. V. Kiew, L. Y. Chung and K. Burgess, *Chem. Soc. Rev.*, 2013, **42**, 77-88; (b) M. Wang, M. G. H. Vicente, D. Mason and P. Bobadova-Parvanova, *ACS Omega*, 2018, **3**, 5502-5510.
20. (a) U. Kragh-Hansen, *Front. Mol. Biosci*, 2018, **5**; (b) J. Wang, V. Yadav, A. L. Smart, S. Tajiri and A. W. Basit, *Mol. Pharm.*, 2015, **12**, 966-973.
21. S. Ntshangase, A. Shobo, H. G. Kruger, A. Asperger, D. Niemeyer, P. I. Arvidsson, T. Govender and S. Baijnath, *Xenobiotica*, 2018, **48**, 938-944.
22. Y. Xiao, Q. Zhang, Y. Wang, B. Wang, F. Sun, Z. Han, Y. Feng, H. Yang, S. Meng and Z. Wang, *Theranostics*, 2018, **8**, 3111-3125.
23. S. Zhu, J. Zhang, J. Janjanam, J. Bi, G. Vegesna, A. Tiwari, F.-T. Luo, J. Wei and H. Liu, *Anal. Chim. Acta*, 2013, **758**, 138-144.
24. A. Hielscher, *Med. Phys*, 2005, **32**, 2096-2096.
25. Y. Gai, Y. Jiang, Y. Long, L. Sun, Q. Liu, C. Qin, Y. Zhang, D. Zeng and X. Lan, *Mol. Pharm.*, 2020, **17**, 349-358.
26. K. Braun, M. Wiessler, R. Pipkorn, V. Ehemann, T. Bauerle, H. Fleischhacker, G. Muller, P. Lorenz and W. Waldeck, *Int. J. Med. Sci.*, 2010, **7**, 326-339.
27. I. Szadvari, O. Krizanova and P. Babula, *Physiol. Res.*, 2016, **65**, S441-S453.
28. (a) T. Troy, D. Jekic-McMullen, L. Sambucetti and B. Rice, *Mol. Imaging*, 2004, **3**, 15353500200403196; (b) R. Weissleder and V. Ntziachristos, *Nat. Med.*, 2003, **9**, 123-128.

EXPERIMENTAL

Material and Methods

All reactions were carried under inert (nitrogen) atmosphere. Toluene and tetrahydrofuran were distilled from standard drying procedures using benzophenone and sodium while the DMSO was dried over calcium hydride and kept over molecular sieves (4 Å). Glutaric anhydride, boron trifluoride diethyl etherate, triethylamine, *N,N'*-disuccinimidyl carbonate, diethylaminomethyl-polystyrene, and fluorescein free acid were purchased from Sigma Aldrich and used without further purification. 2,4-dimethylpyrrole was obtained from DLD Scientific (South Africa) and it was used as received. The c(RGDyK) was purchased from FutureChem Co, Ltd (Seoul, Korea) and it was used as received. All solvents such as ethanol, DMF, DMSO, DCM and TFA were of HPLC-grade and were all purchased from Sigma Aldrich. The synthesis of dipyrromethene intermediate (Compound **3**) was performed using CEM Discovery SP-microwave reactor, USA. The reactions were monitored using a Thin Layer Chromatography (TLC) Merck 60 F_{254} silica gel aluminium coated sheets and using LC-MS analysis was carried out (Shimadzu 2020 UFLC-MS, Japan), with the following conditions: column: YMC-Triat C18 (150 x 4.6 mm, 5 µm), equipped with a photodiode array detector, SPD-MZOA model and the mobile phase: 0.1 % formic acid in water and acetonitrile operating in gradient mode (5-95% in 9 minutes with a hold for 9 minutes or 5-95% in 15 minutes with a hold for 5 minutes). The compounds that were purified with gravity column chromatography made use silica with mesh particle size, 40-63 µm. For compounds that were purified using SFC were carried out on Sepiatec Prep SFC basic (Germany). All reactions were performed in duplicate. The ^{1}H, ^{13}C , ^{19}F NMR spectra were recorded on Bruker AVANCE III 400 MHz at room temperature and the chemical shifts were reported relative to deuterated chloroform (δ = 7.26 ppm). High-Resolution Mass Spectra (HRMS) were obtained from Bruker micro-TOF-Q II instrument at ambient temperatures, sample concentration of 1 µg/ml. Optical Imaging was performed using the IVIS Lumina III equipment (Perkin Elmer, USA) at the Preclinical Imaging Facility (Pelindaba, South Africa).

Spectroscopic measurements

Absorption spectra were recorded on the UV-3600 Shimadzu UV-VIS-NIR spectrophotometer with the slit width of 2 nm and the pathlength of the cuvette was 1.0 cm. The fluorescent emission spectra were recorded on the PerkinElmer LS 55 fluorescence spectrophotometer. The fluorescence quantum yield of the synthesized BODIPY derivatives were determined by comparing the absorption and emission spectra of BODIPY derivatives prepared as ethanol solutions (refractive index 1.361) with the standard fluorescein prepared in 0.1 M NaOH solution (refractive index 1.330). As per literature the fluorescent quantum yield for standard fluorescein is reported to be of 0.85.[2] The stock solutions concentration of 5.0×10^{-4} M were prepared and diluted to 5.0×10^{-6} M which was then diluted to suitable concentrations for the collection of the absorbance and the emission spectra. Measurements obtained for calculating the molar absorptivity and fluorescent quantum yield were taken from the prepared solutions with the concentration between 0.25×10^{-6} M to 1.50×10^{-6} M. These solutions provided the absorbance values that were below 0.11 at each λmax. The absorbance that is below 0.11 is essential to avoid auto-absorbance and false results. The molar absorptivity and fluorescent quantum yield were calculated according to the following equations; (equation 1 and equation 2).

$$\mathbf{A = \varepsilon \times b \times c} \qquad \textbf{(Equation 1.1)}$$

$$\mathbf{\phi_x = \phi_{st}} \left(\frac{\mathbf{Grad_x}}{\mathbf{Grad_{st}}}\right)\left(\frac{\eta_x^2}{\eta_{st}^2}\right) \qquad \textbf{(Equation 2)}$$

Examples

1. **Determining the molar absorptivity coefficient (ε)**

Plot the concentration against the absorbance at λmax of the prepared solutions to find the slope

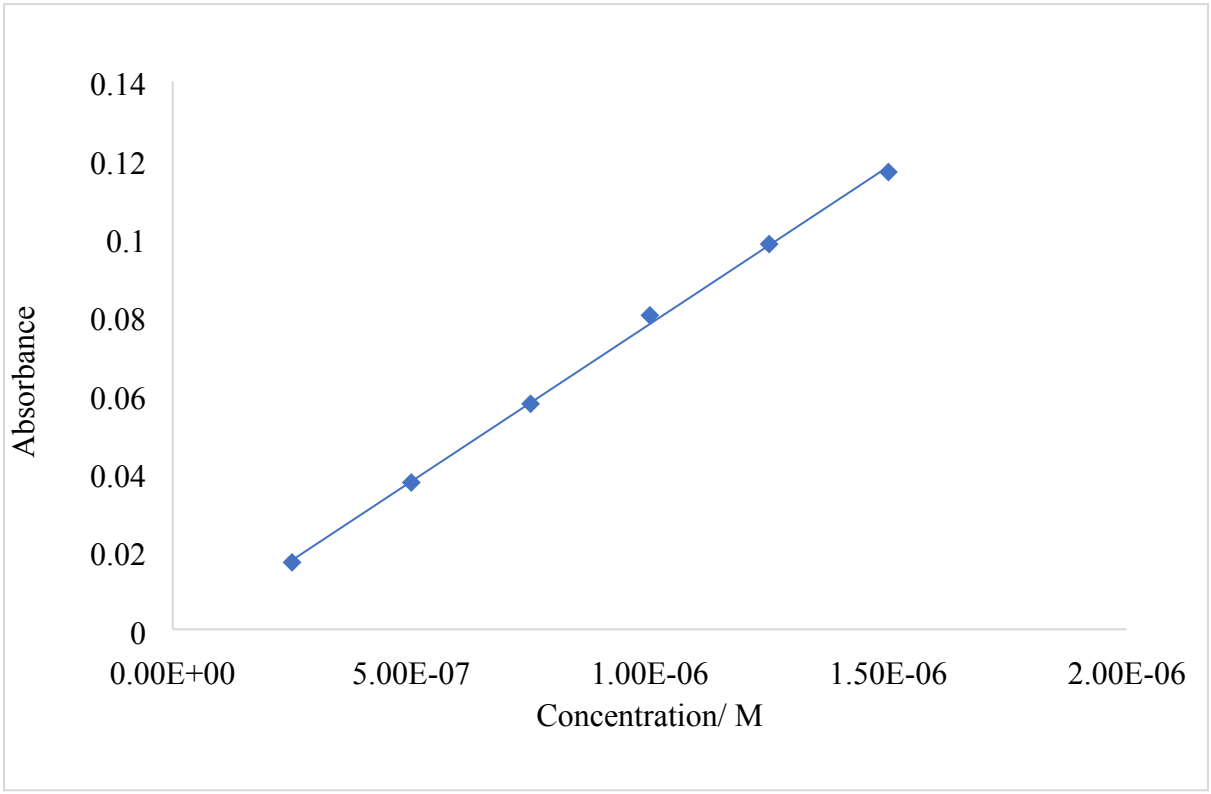

Figure 1 : Plot of Meso-carboxyl BODIPY (**Compound 4**) concentration against the absorbance, solutions prepared in ethanol.

Pathlength b = 1 cm

Then rearrange **equation 1** to $\boldsymbol{\varepsilon = \frac{A}{C} \times b}$, which is equal to the slope of the curve

Therefore; $\boldsymbol{\varepsilon = 80434\ M^{-1}.cm^{-1}}$

2. Determining the fluorescent quantum yield

Plot the emission versus the absorbance for the samples and the standard to find the slopes

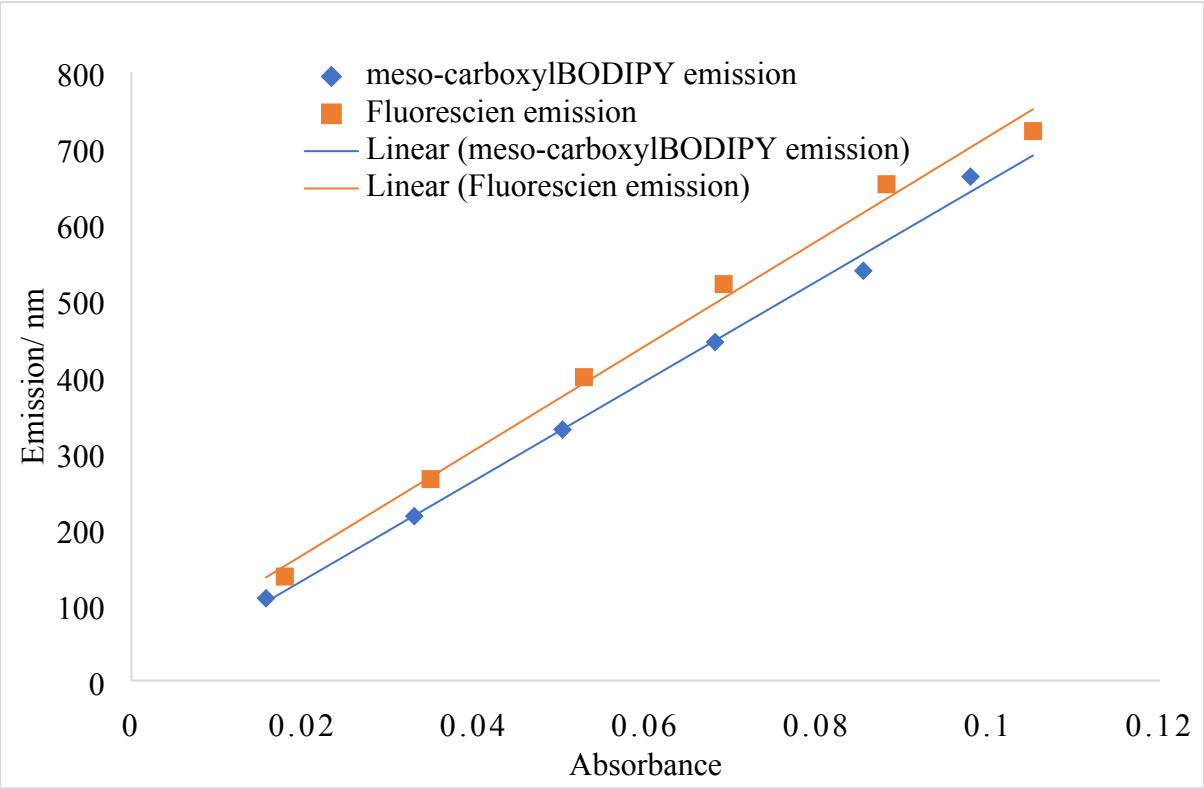

Figure 2: Plot of absorption vs emission for the meso-carboxyl BODIPY (sample/ x) and fluorescein (standard/ st)

Standard fluorescein quantum yield = 0.85

Plug in values to equation 2.

$$\phi_f = \mathbf{0.8500}\left(\frac{\mathbf{6558}}{\mathbf{6877.3}}\right)\left(\frac{\mathbf{1.361^2}}{\mathbf{1.330^2}}\right)$$

$$\phi_f = \mathbf{0.8487}$$

The same procedure was applied for all the other compounds and the results are presented in **Table 1.**

Table 1: Photophysical properties of *meso*-carboxyl BODIPY dye (**4**), *meso*-BODIPY-NHS (**8**) and BODIPY peptides (**9-11**) in ethanol.

Compound	**λmax(abs)/ nm**	**λmax (em)/ nm**	**Δλ/ nm**	**ε / $M^{-1}.cm^{-1}$**	**ϕ_f**
4	495	504.5	9.5	80434	0.849
8	498	506.0	8.0	75943	0.581
9	496	504.5	8.5	33383	0.609

10	497	505.5	8.5	37189	0.525
11	495	505	10	3716.3	0.508

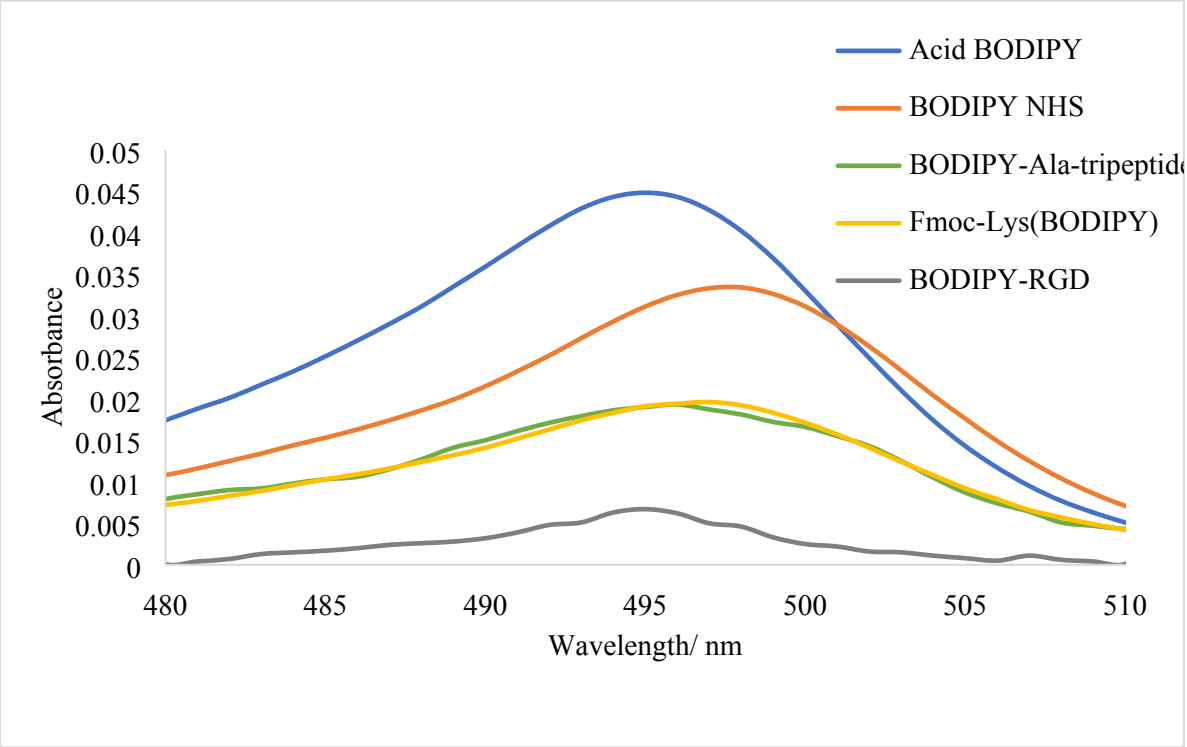

Figure 3: Absorption spectrum of *meso*-carboxyl BODIPY dye, *meso*-BODIPY-NHS and BODIPY peptides (0.5 µM) in ethanol.

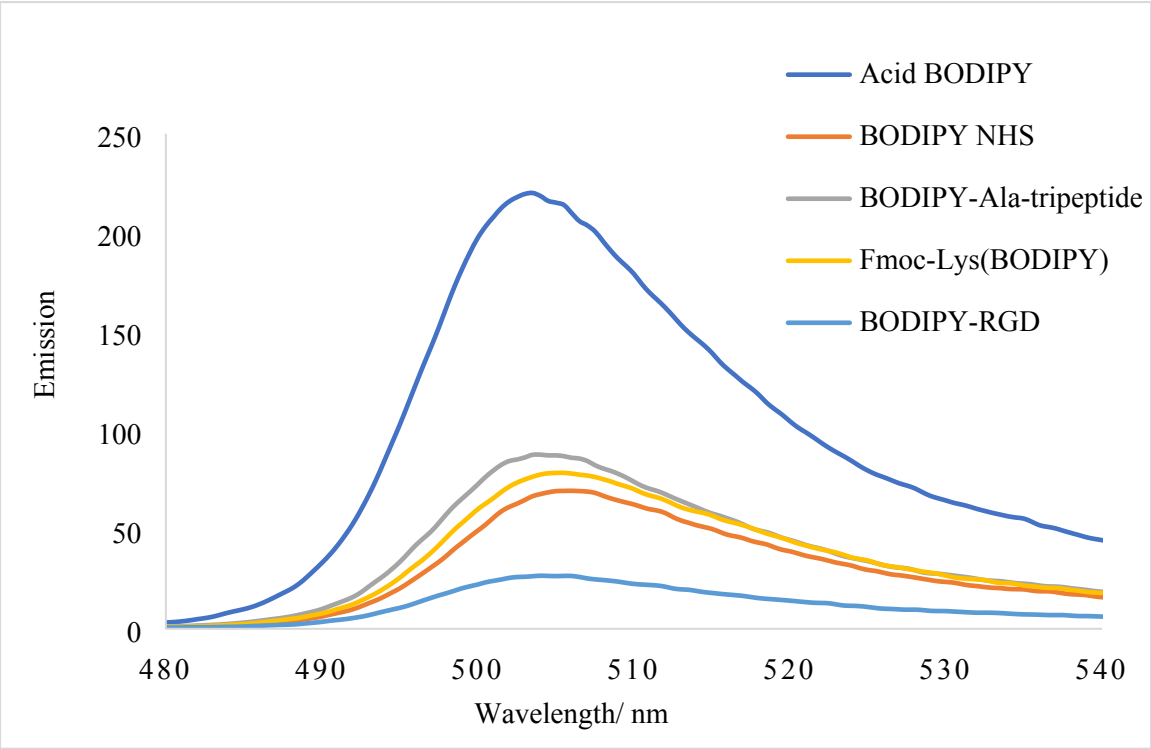

Figure 4: Emission spectrum of *meso*-carboxyl BODIPY dye, *meso*-BODIPY-NHS and BODIPY peptides (0.5 µM) in ethanol.

BODIPY-c(RGDyK) serum stability

Untreated plasma was obtained from Sprague-Dawley rats and stored at -80 °C. On sample preparation, 990 µL of serum was spiked with 10 µL of 1 mg/mL BODIPY-c(RGDyK), homogenised and incubated at room temperature over a maximum of 4h. A previously published method was employed to obtain and prepare samples at 0 h and thereafter hourly for analysis.[1] Briefly, 100 µL of spiked serum was diluted with 900 µL methanol (MeOH), subjected to vigorous mixing for 1 min and centrifuged at 12000 rpm for 15 min at 4 °C. The supernatant was filtered through the hydrophilic-lipophilic balance (HLB, Sigma Aldrich) cartridge as follows: the cartridge matrix was conditioned first with ACN (2 ×1 mL) followed by MeOH (2 ×1 mL). The supernatant (~1 mL) was then loaded onto the cartridge and the flow-through was collected into an HPLC vial until the cartridge was dry. The eluent was mixed well and injected on a Thermo Scientific™ | UltiMate™ 3000 UPLC system coupled to Bruker Amazon Speed-Ion Trap Mass Spectrometer with the following separation and detection parameters. The LC separation was achieved using biphenyl 2.7 µm column (50 × 4.6 mm). The mobile phase were ultra-pure water (0.1 % v/v FA) and acetonitrile (0.1 % v/v FA) at 0.35 mL/min for 10.1 min with the column compartment set to room temperature in the gradient mode of separation. The MS acquisition parameters were positive ion trap

polarity with the endplate offset and the capillary voltage of 600 V and 5000 V. The nebuliser pressure was 1.5 bar and the dry gas was flowing at a flow rate of 8 L/min. Dry heater temperature was 200 °C and the scan range was from m/z 600 to 1100.

Characteristics of the fluorescence signal for BODIPY-c(RGDyK)

In preparation for image acquisition a BODIPY-RGD concentration of 21 nmol/mL for injection) was tested for fluorescence intensity. A manufacture-proposed present for optical imaging using an excitation (ex) at 480 nm paired with emission (em) at 570 nm yielded counts for subsequent BODIPY-RGD injection that were sufficient and well within the allowable count range (minimum of 600 and maximum of 60000) supported by the apparatus calibration. This related to a maximum radiant efficiency of 7.7 x 10^9 (p/sec/cm^2/sr)/μW/cm^2 (**Figure 5**). Testing of the formulated injection solution included fluorescence image acquisition of a 1 mL plastic syringe carrying 0.3 mL stock solution of BODIPY-RGD (6 nmol); images were acquired with the same camera settings to warrant comparison. Image acquisition was comparing the available filter pairs to determine the peak fluorescence (**Figure 6**).

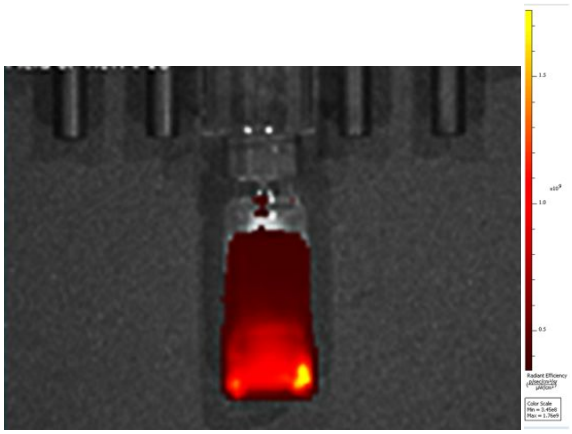

Figure 5: Imaging of BODIPY-c(RGDyK): diluted (21.0 μM). Image acquisition: Lumina IVIS III; exposure time-0.5 s, binning factor -8, F/stop- 2, field of view-10 cm, Ex 480 nm and Em 570 nm

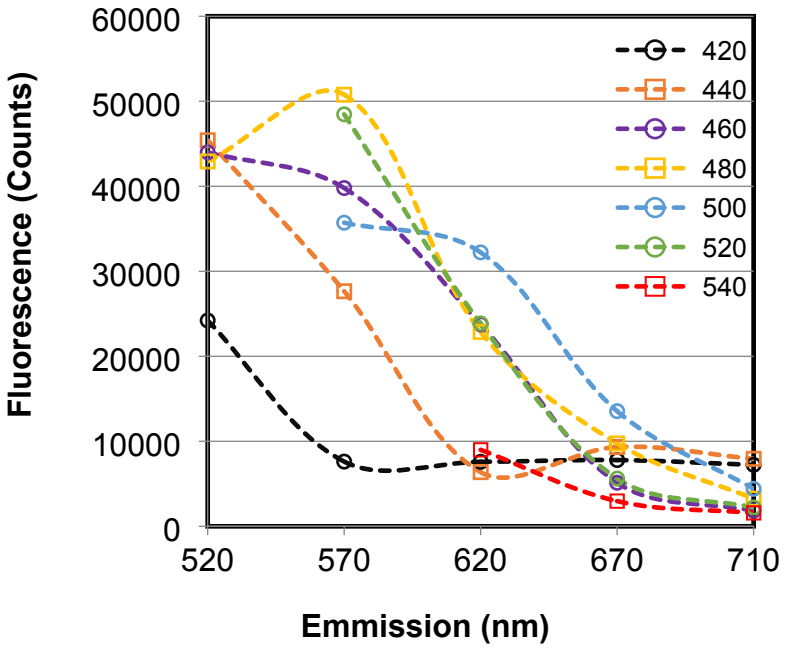

Figure 6: Characterization of BODIPY-c(RGDyK) fluorescence for *in vivo* optical imaging. Image acquisition of BODIPY-c(RGDyK) was performed using IVIS Lumina III of a 1 mL plastic syringe carrying 0.3 mL (6 nmol) BODIPY-c(RGDyK (exposure time: 0.5 sec, binning factor: 8,f/stop:2.0, field of view:10 cm); Legend shows the different excitation wavelengths (available filters of the apparatus).

BODIPY-c(RGDyK)-based Fluorescence Imaging *in vivo*

Eight weeks-old female BALB/c nude (nu/nu) mice of were provided the Preclinical Drug Development Platform Viviarium (North West University, Potcheftroom), acclimatized and handled according to the national standards of animal care. All animal experiments were performed in compliance with the North West University's (South Africa) policy on animal use and ethics. The North West University AnimCare Ethics committee granted the ethical clearance with ethics number NWU-00184-18-A5. Three wild type mice were used as control and another two mice were inoculated with MCF-7 – a metastatic breast cancer cell line. At 3-4 weeks after inoculation tumor reached a diameter of approximately 7.5 mm. Tumor dimensions were measured using a calliper, the tumor volume was calculated using the equation: volume (V) = length × width^2/2. No particular animal preparation was required leading up to the administration of BODIPY-c(RGDyK (1.5-3 nmol/150 µL) which was injected via the tail vein. The mice were anesthetized using 2% isoflurane carried in an oxygen/air mixture and whole body images were acquired at 3 h and 24 h post injection

BODIPY-c(RGDyK)-based Fluorescence Imaging *ex vivo*

To eradicate interference from the background, *ex vivo* imaging measures were performed also using the optical imaging instrument. Following the final image acquisition mice were euthanized by cervical dislocation. Following blood drainage animal dissection was performed; tumors and multiple organs (heart, liver, spleen, bone, muscle, brain, lung and kidneys) were harvested for excised organ image acquisition using the same in vivo imaging equipment and procedures.

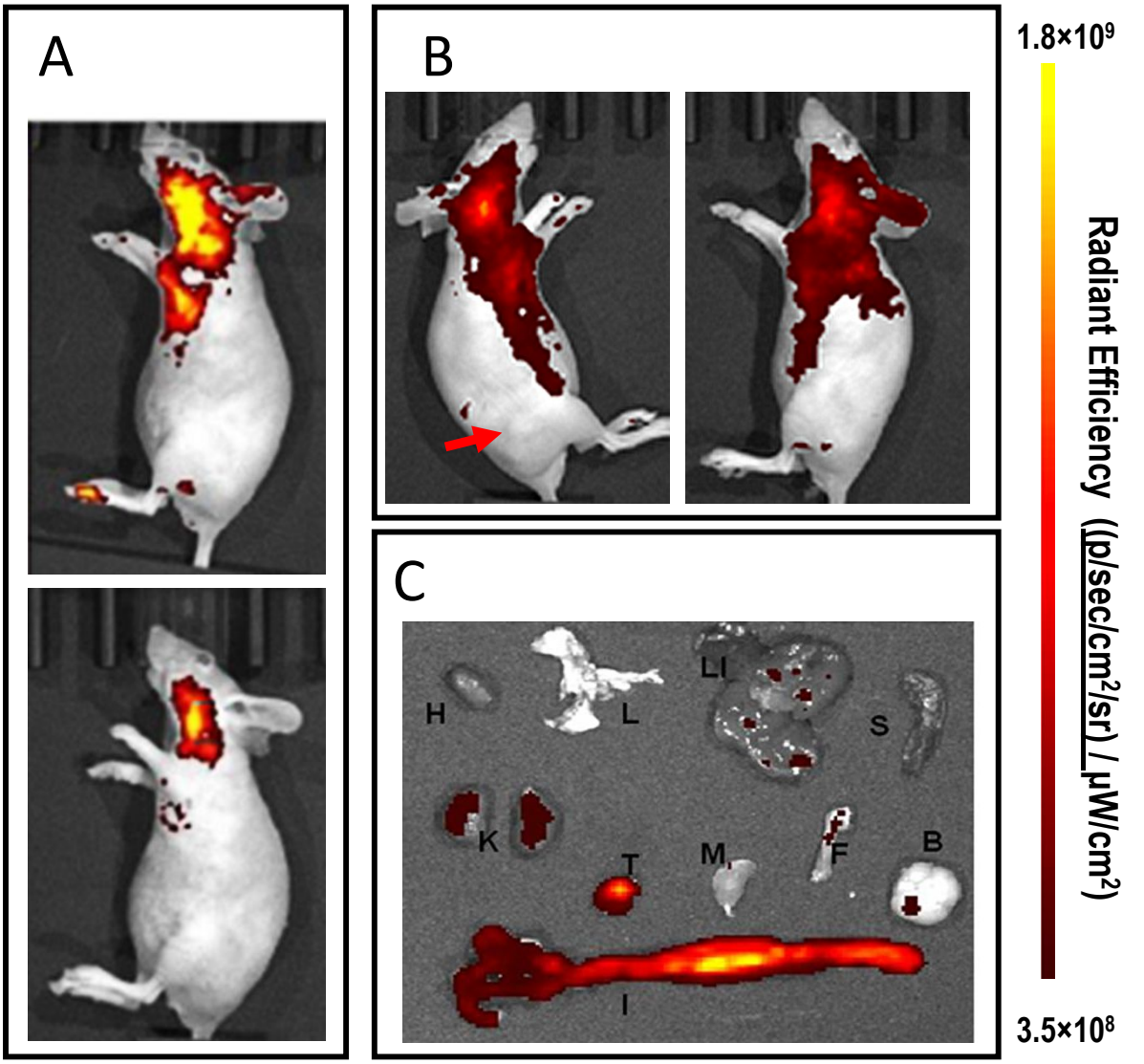

Figure 7: Overview of BODIPY-c(RGDyK) Fluorescence Imaging
Animals received a 0.15 mL bolus of BODIPY-c(RGDyK) via tail vein injection. Image were acquired (field of view =10.0 - 12.5 cm; Level=high, Ex/Em filter pair (nm) = 480/570) using IVIS Lumina III (Perkin Elmer, Rodgau, Germany) and fluorescence signals were displayed over bright light photos of animals, organs or tissue using Living Image Software 4.5.5 (Perkin Elmer, Rodgau, Germany). Imaged are corrected for background (counts < 600) and injected dose. (**A**) Representative images of a wild type balb /c mouse showing BODIPY-c(RGDyK) fluorescence signal (radiant efficiency) *in vivo* at 3 h (top) and 24 h (bottom) following intravenous probe injection; image exposure time (sec) /binning/ f-stop = 0.5/ 8/

2.0. (**B**) *In vivo* tumour visualization of a representative balb/c mouse bearing a MCF-7 tumor xenograft (red arrow indicates tumor location) in the hind flank (left image) compared to the contralateral side (without tumor; right image); image exposure time (sec) /binning/ f-stop = 0.5/ 8/ 2.0. (**C**) Qualitative *ex vivo* organ and tissue analysis; representative biodistribution at 24 h after administration (image exposure time (sec)/ binning/ f-stop = 2.0/ 8/ 2.0). Displayed organ/tissues are: H= heart, L=lung, LI=liver, S=spleen, K=kidneys, T- =tumour, M=muscle, F= femur (bone), B=brain and I= intestines.

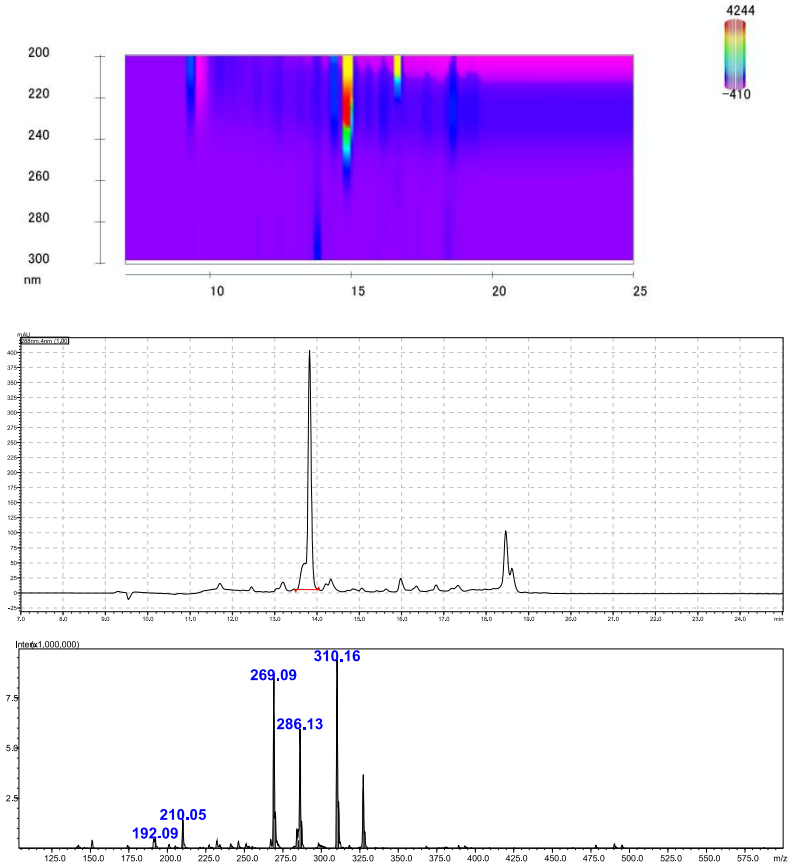

Figure 8: Crude reaction mixture LC-MS-PDA chromatogram of glutaric **3** (~13.8 min) with desired m/z 286 (+ve mode), major UV peak is pyrrole.

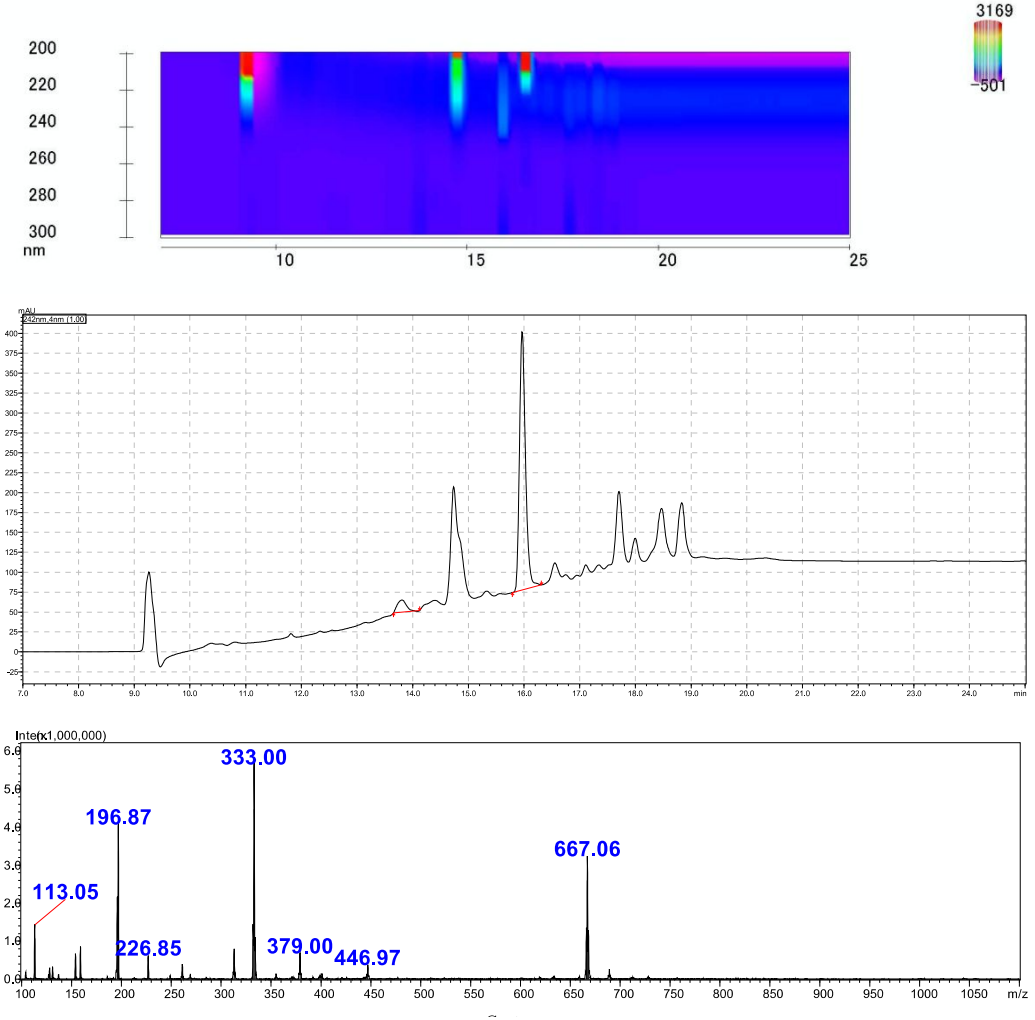

Figure 9: Crude reaction mixture LC-MS-PDA chromatogram of glutaric **4** (~15.9 min) with desired m/z 333 (-ve mode)

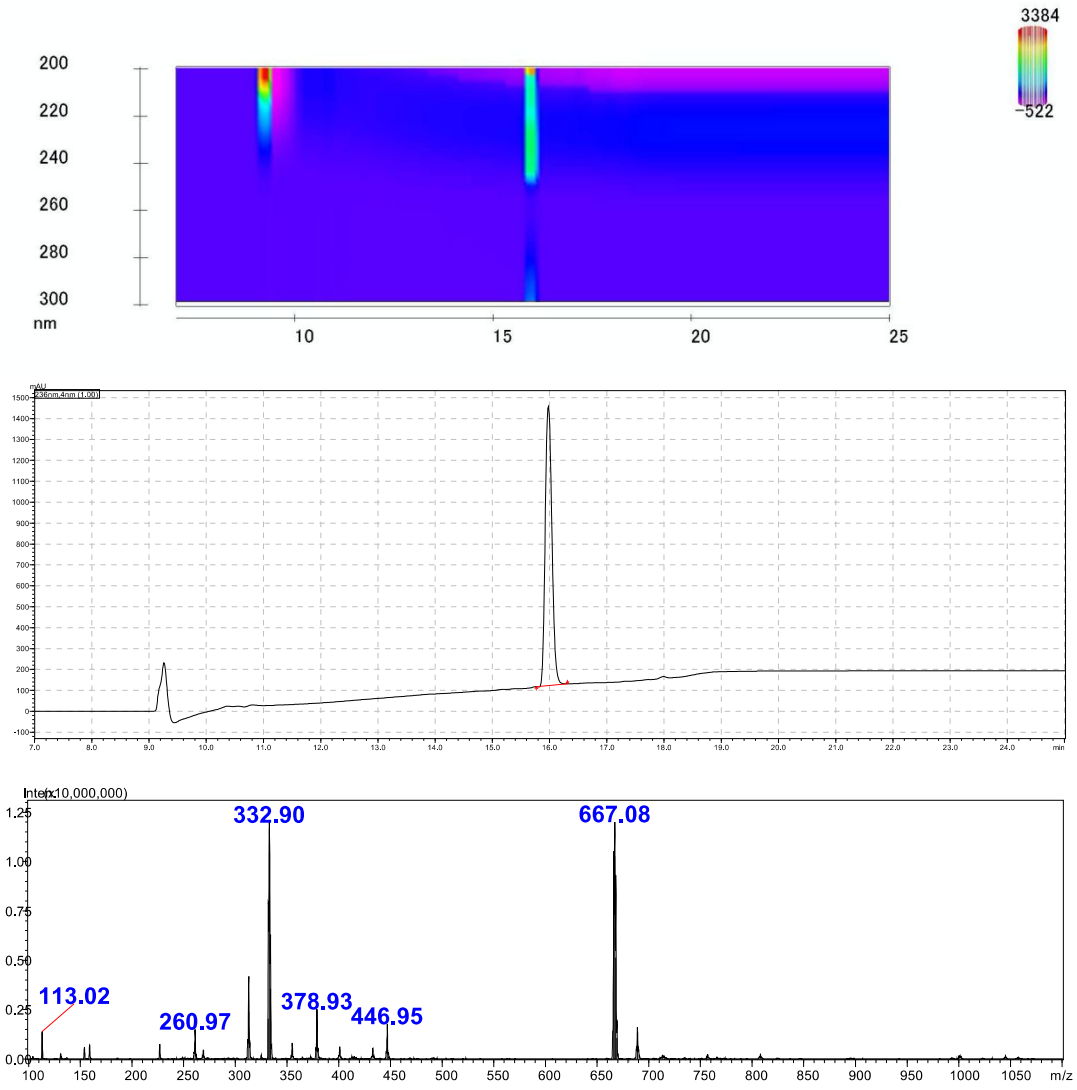

Figure 10: Pure LC-MS-PDA chromatogram of glutaric **4** (~15.9 min) with desired m/z 332.9-333 (-ve mode)

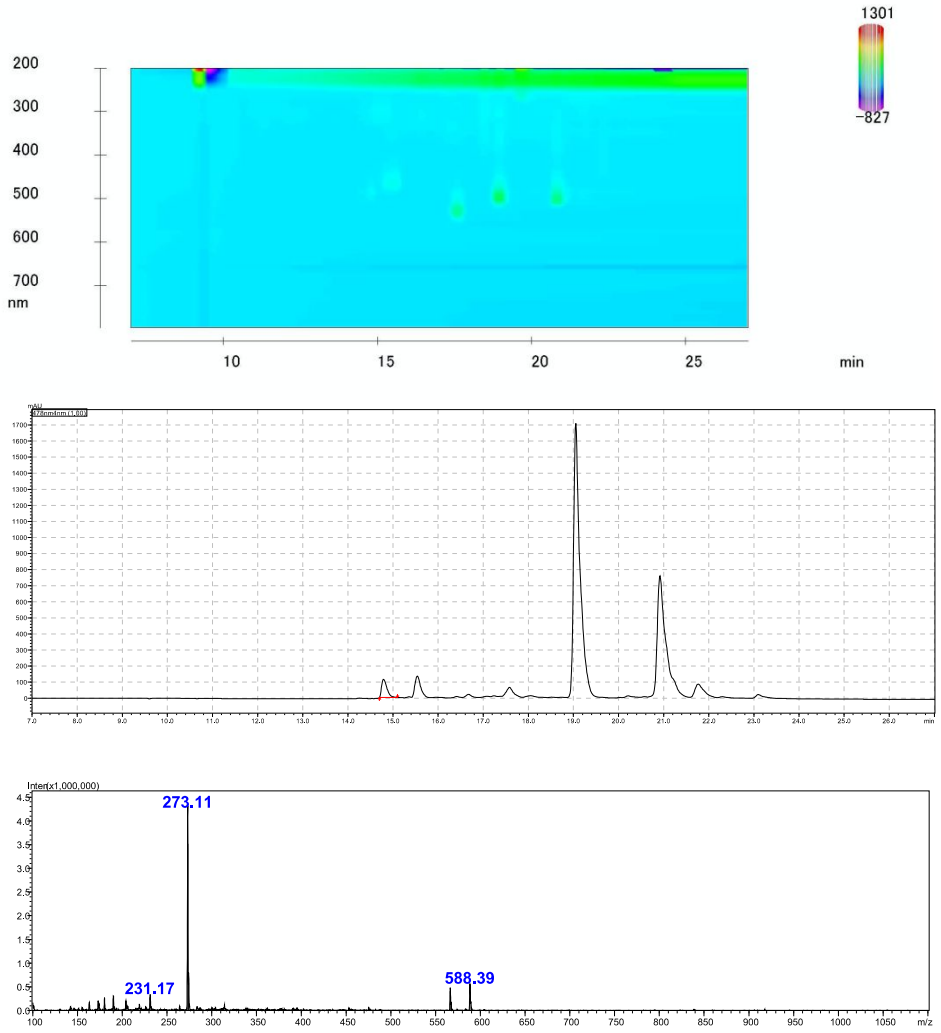

Figure 11: Crude reaction mixture LC-MS-PDA chromatogram of succinic **3** (~14.6 min) with desired m/z 273 (+ve mode)

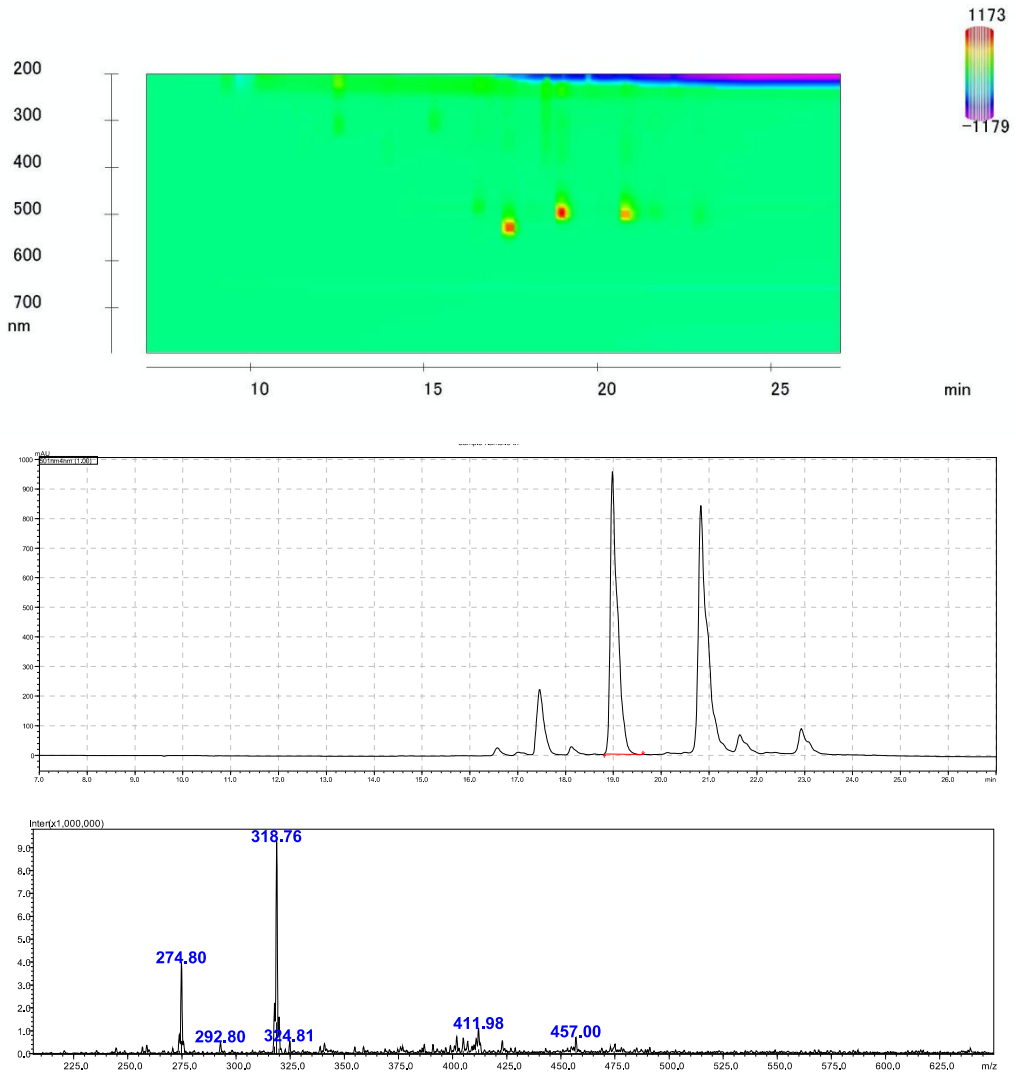

Figure 12: Crude reaction mixture LC-MS-PDA chromatogram of succinic **4** (~19.0 min) with desired m/z 318-319 (-ve mode)

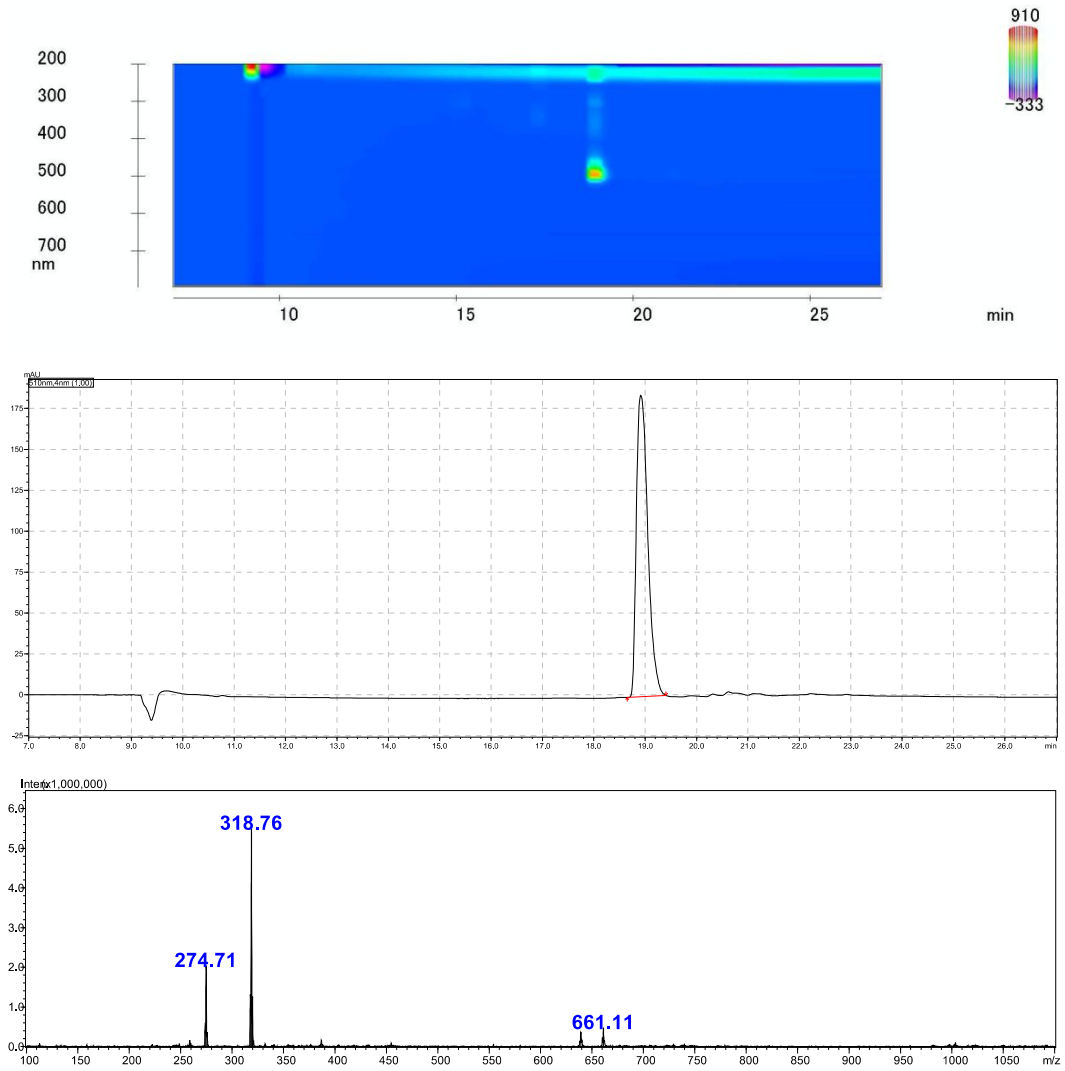

Figure 13: Pure LC-MS-PDA chromatogram of succinic **4** (~19.0 min) with desired m/z 318-319 (-ve mode) or 321 (+ve)

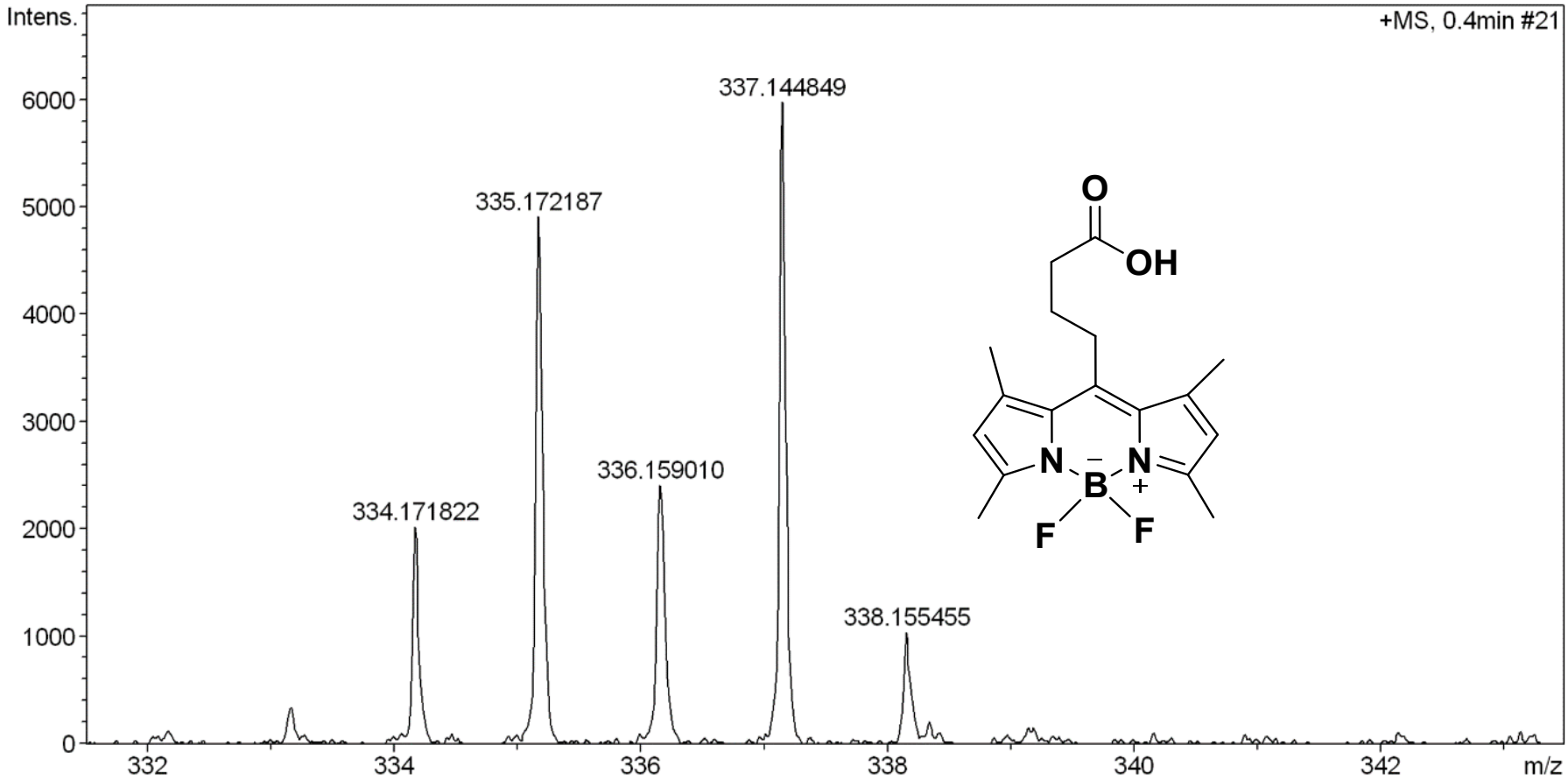

Figure 14: HRMS spectrum for 4-(4,4-Difluoro-1,3,5,7-tetramethyl-4-bora-3a,4a-diaza-s-indacene-8-yl)-butyric Acid (**4)**

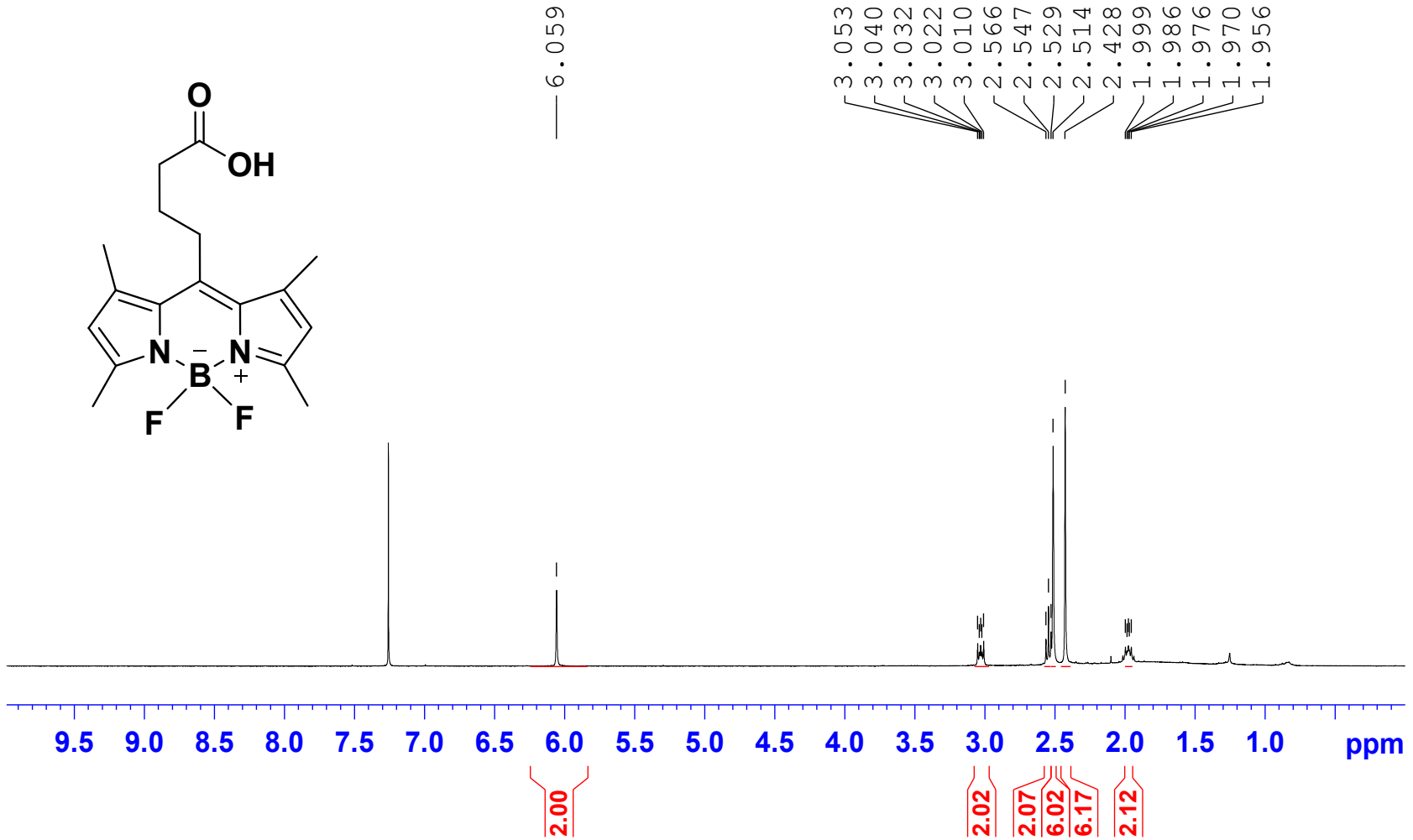

Figure 15: Proton (^{1}H) NMR spectrum of 4-(4,4-Difluoro-1,3,5,7-tetramethyl-4-bora-3a,4a-diaza-s-indacene-8-yl)-butyric Acid (**4**)

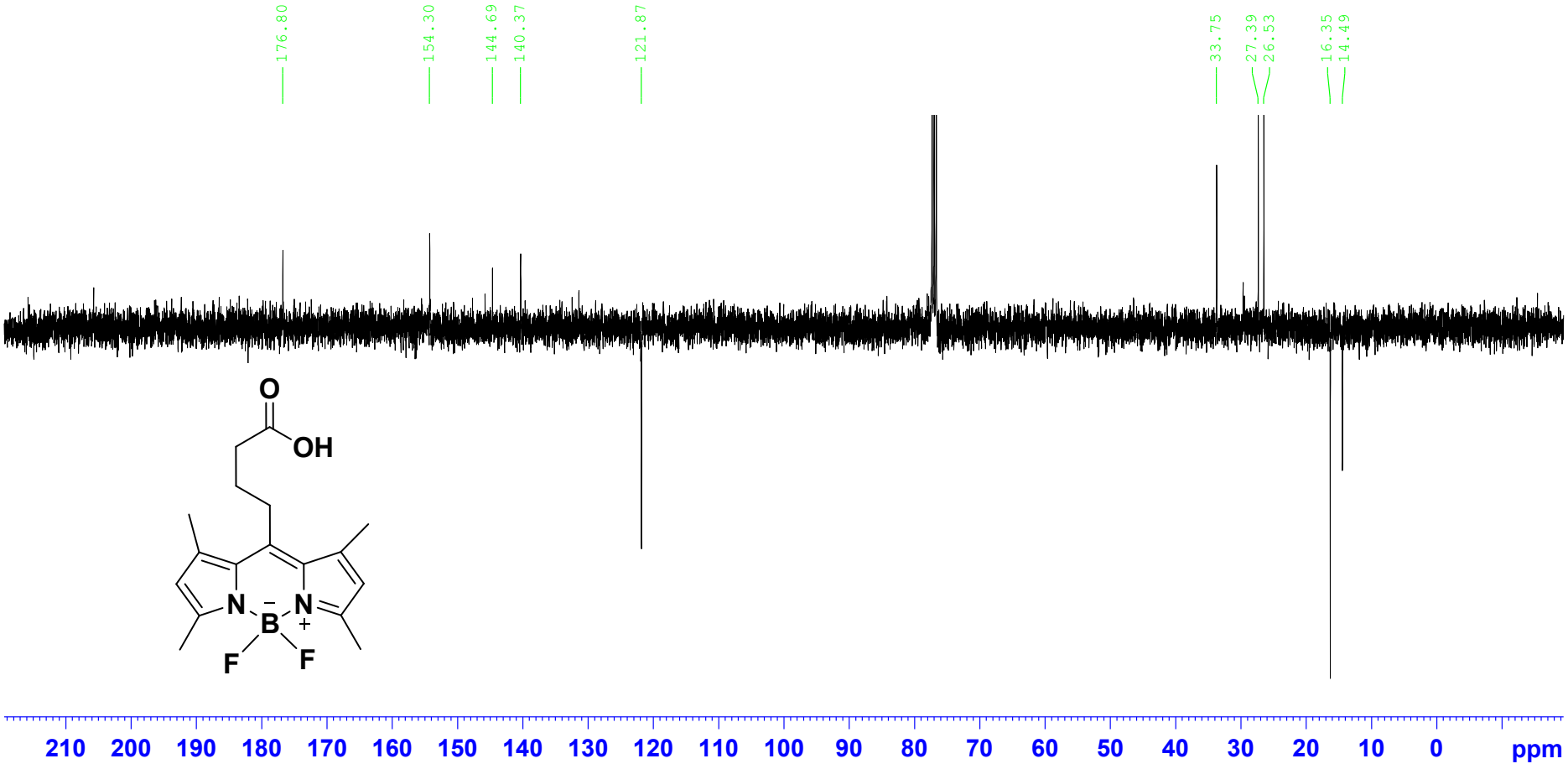

Figure 16: Carbon ^{13}C NMR spectrum 4-(4,4-Difluoro-1,3,5,7-tetramethyl-4-bora-3a,4a-diaza-s-indacene-8-yl)-butyric Acid (**4**)

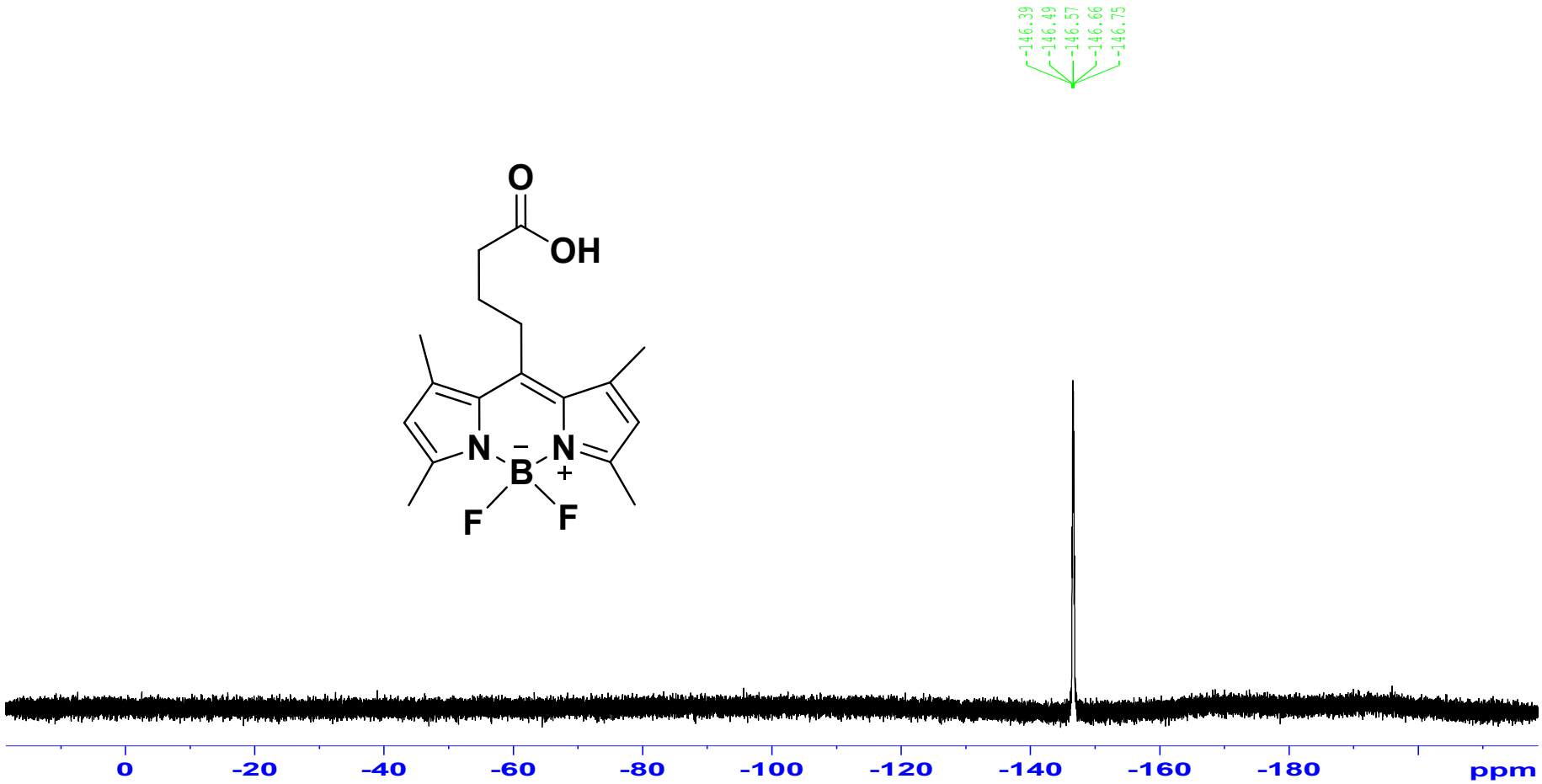

Figure 17: ^{19}F NMR spectrum of 4-(4,4-Difluoro-1,3,5,7-tetramethyl-4-bora-3a,4a-diaza-s-indacene-8-yl)-butyric Acid (**4**)

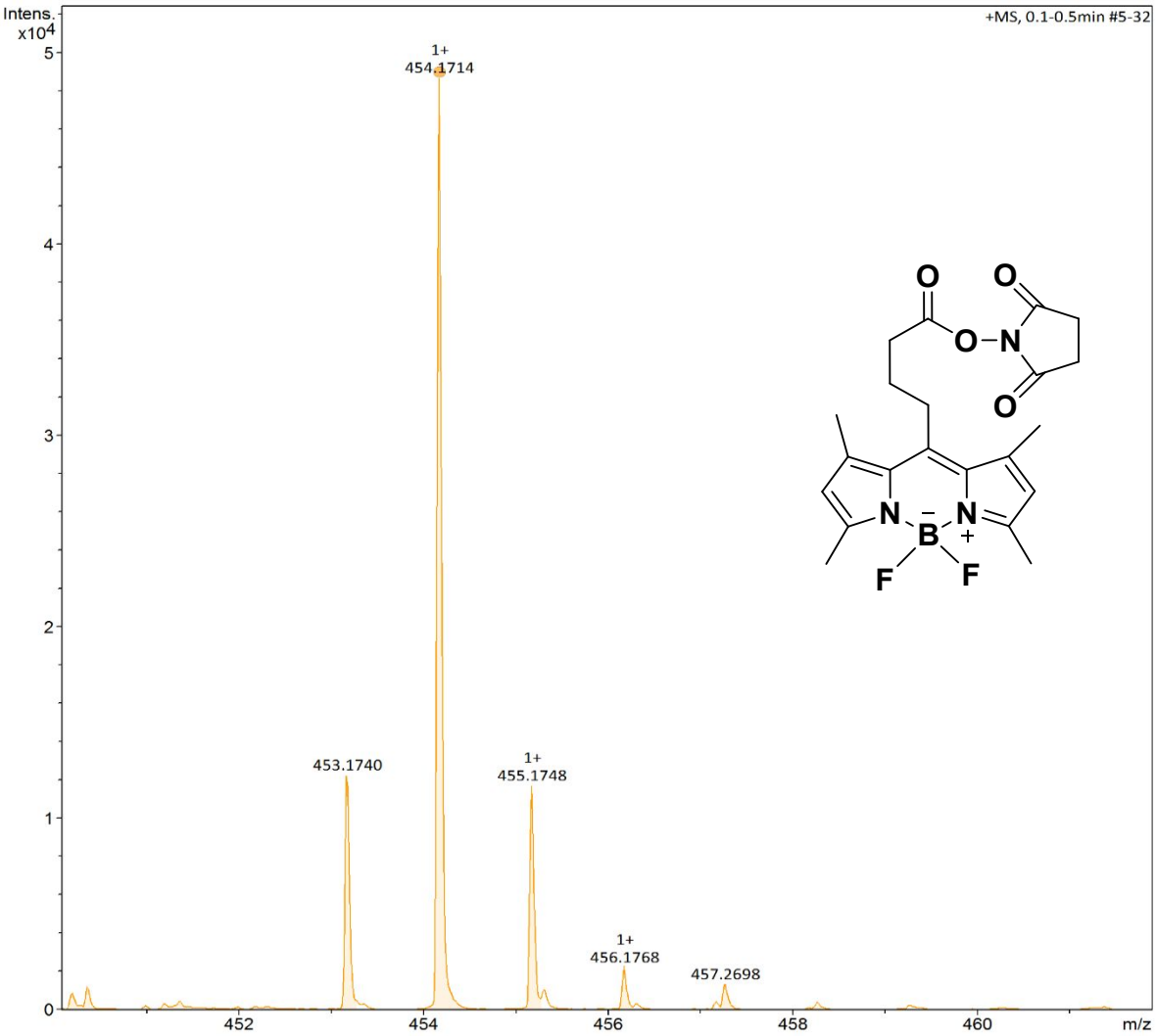

Figure 18: HRMS spectrum for 4-(4,4-Difluoro-1,3,5,7-tetramethyl-4-bora-3a,4a-diaza-s-indacene-8-yl)-butyric succinimidyl Ester (**8**)

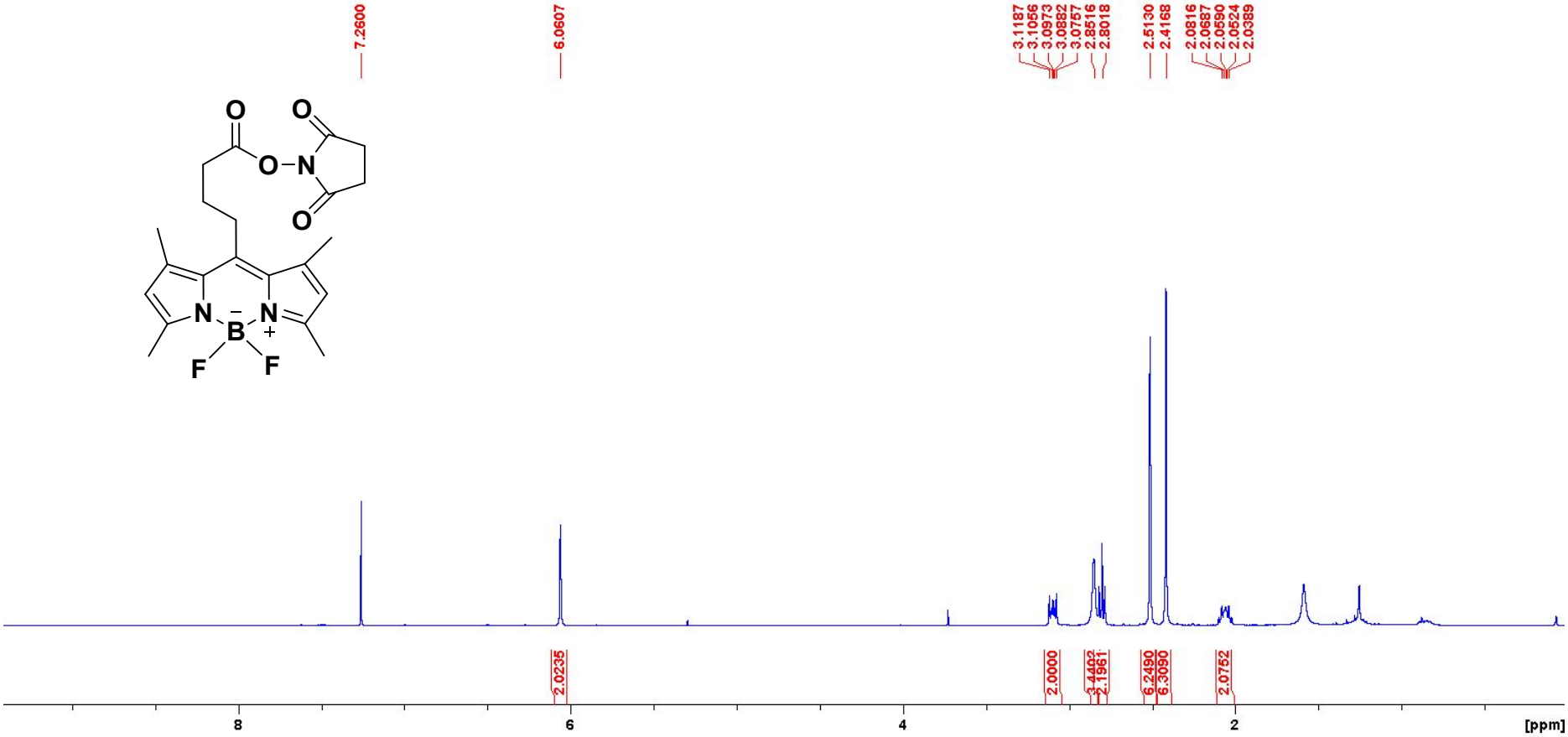

Figure 19: ^{1}H NMR spectrum of 4-(4,4-Difluoro-1,3,5,7-tetramethyl-4-bora-3a,4a-diaza-s-indacene-8-yl)-butyric succinimidyl Ester (**8**)

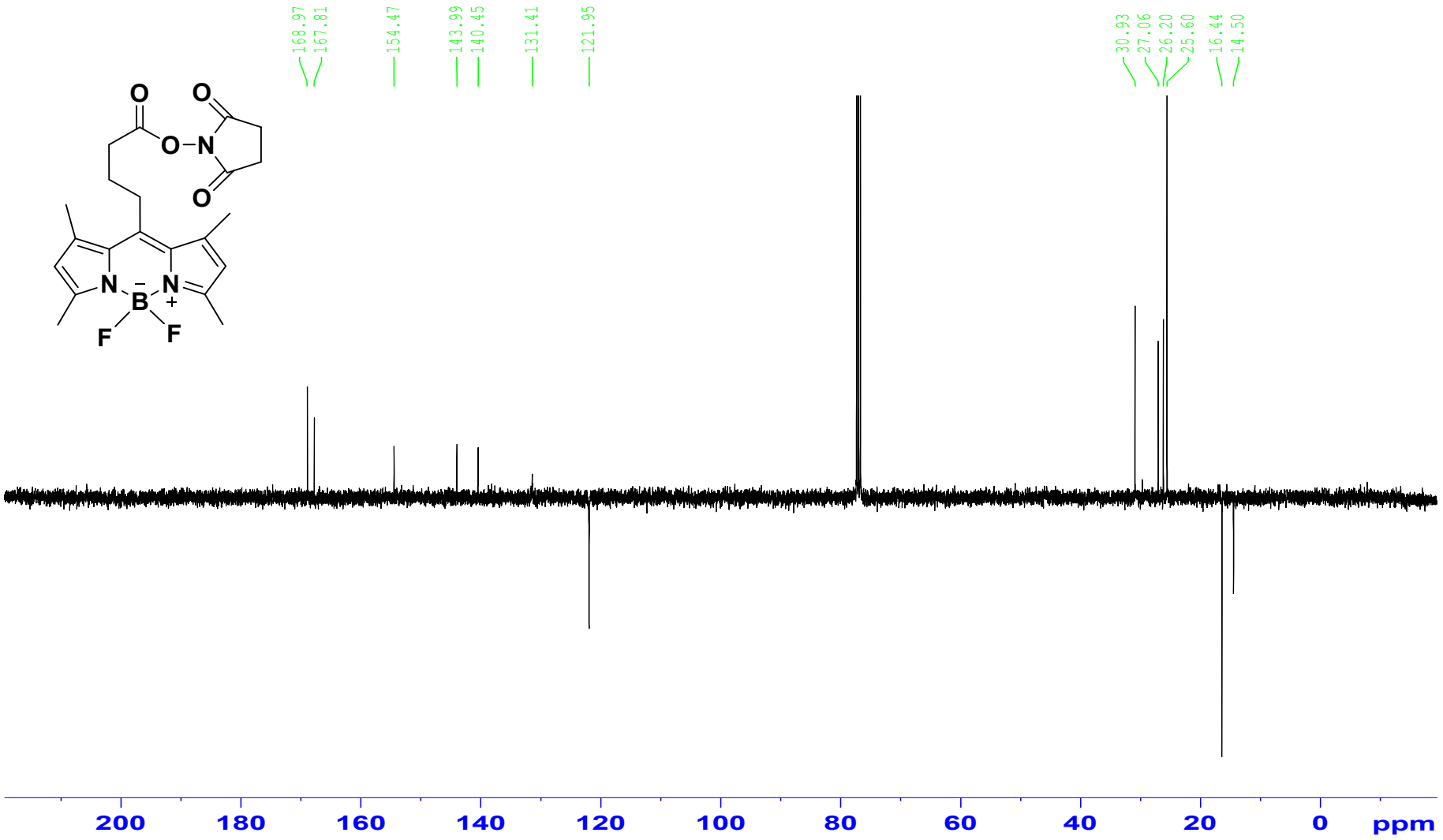

Figure 20: ^{13}C NMR spectrum of 4-(4,4-Difluoro-1,3,5,7-tetramethyl-4-bora-3a,4a-diaza-s-indacene-8-yl)-butyric succinimidyl Ester (**8**)

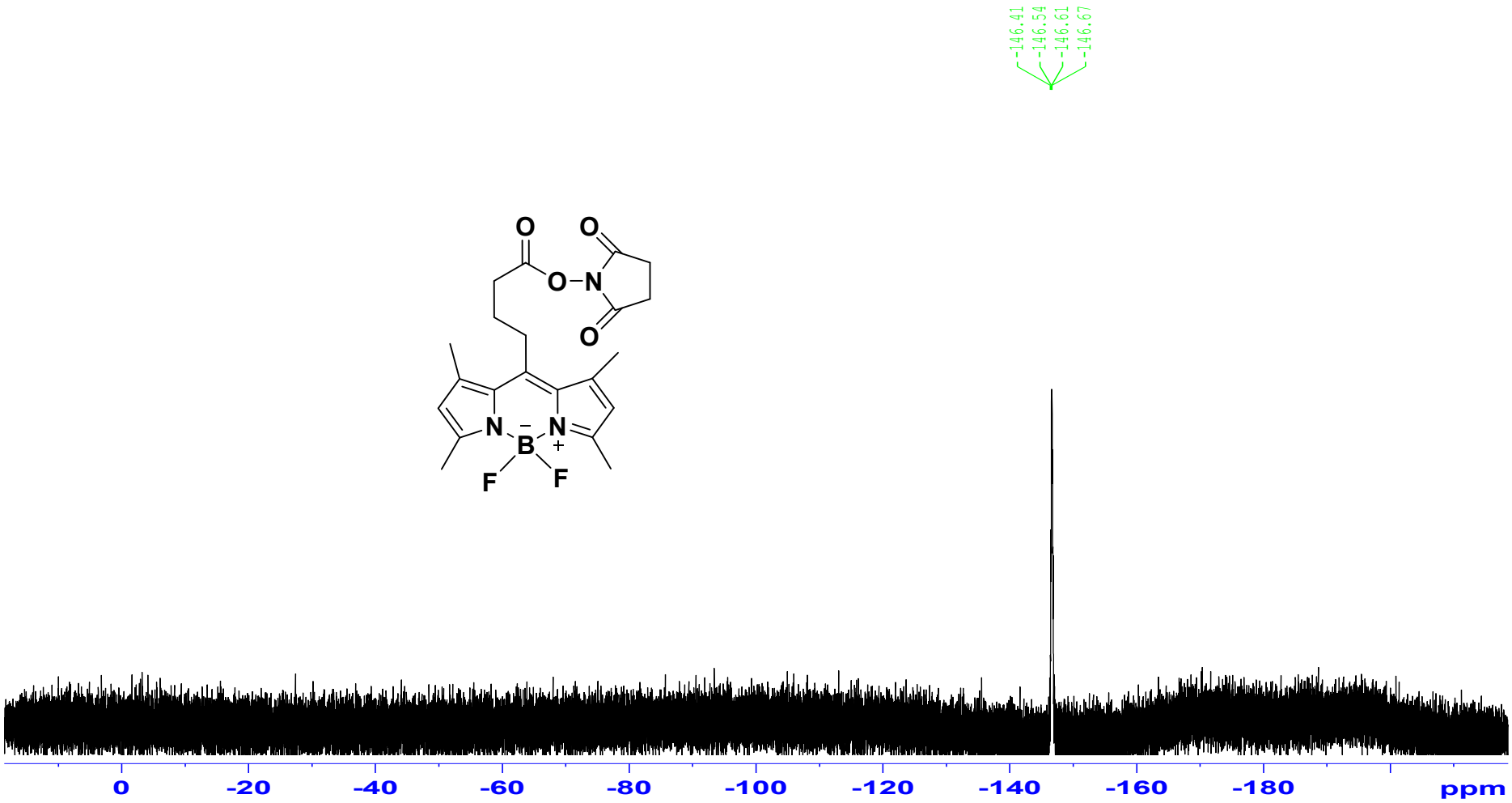

Figure 21: ^{19}F NMR spectrum of 4-(4,4-Difluoro-1,3,5,7-tetramethyl-4-bora-3a,4a-diaza-s-indacene-8-yl)-butyric succinimidyl Ester (**8**)

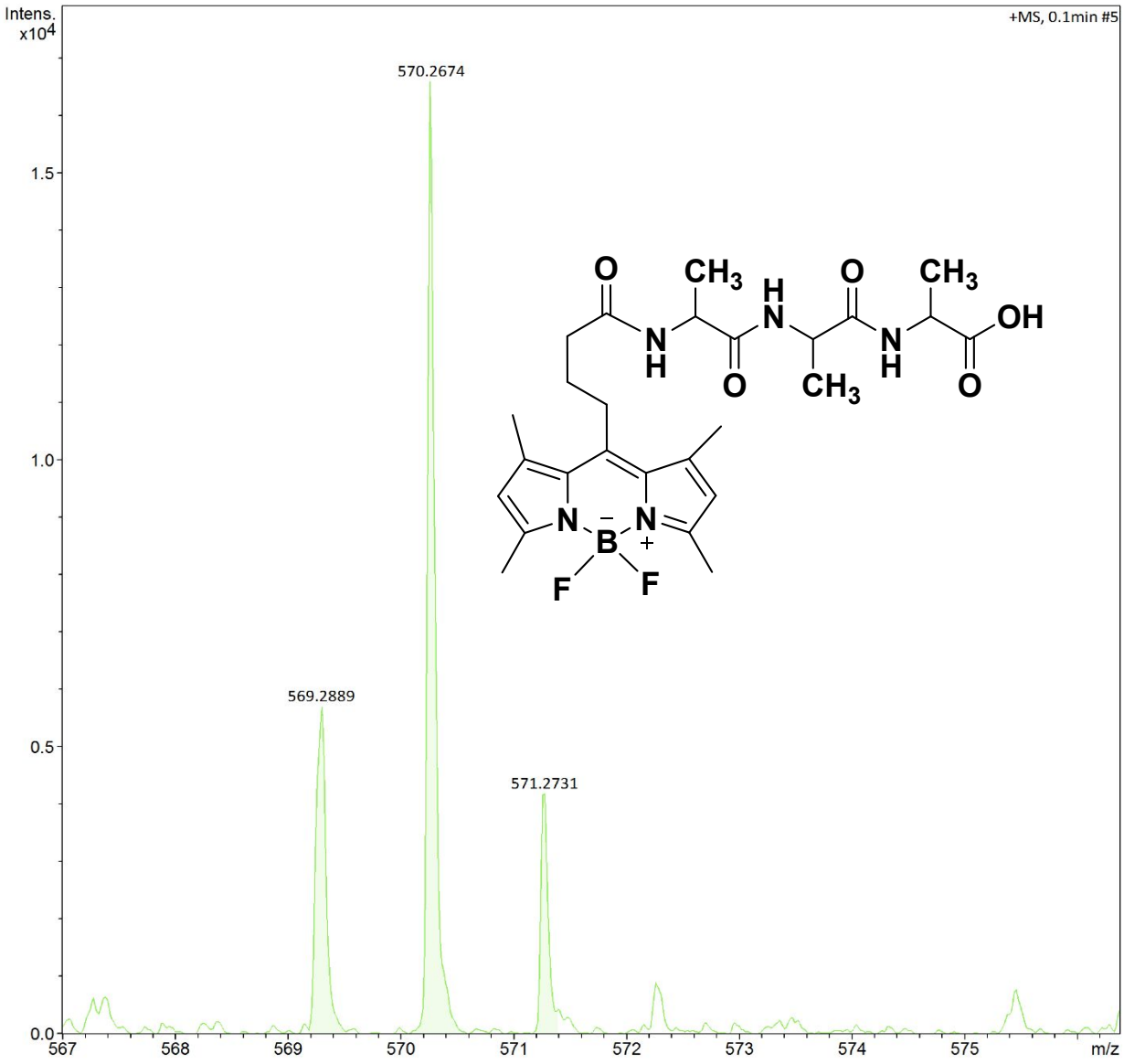

Figure 22: HRMS spectrum for 4-(4,4-Difluoro-1,3,5,7-tetramethyl-4-bora-3a,4a-diaza-s-indacene-8-yl)-butyricamide-Ala-tripeptide (**9**) with Na^+ adduct.

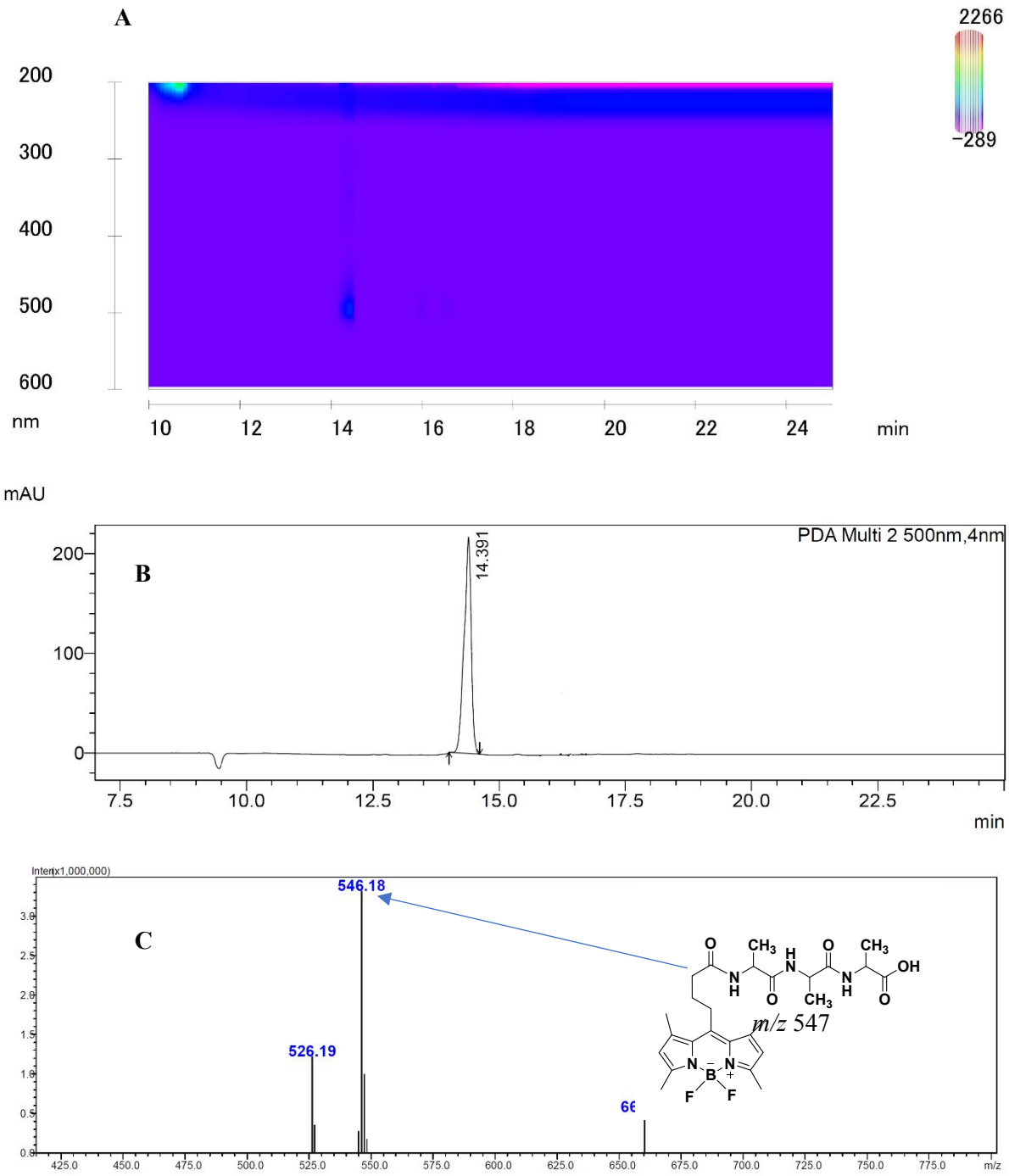

Figure 23: LC-MS-PDA chromatogram of **9. A** PDA showing the purity, **B** LC with retention time and **C** is the MS with the mass in $[M-H]^-$

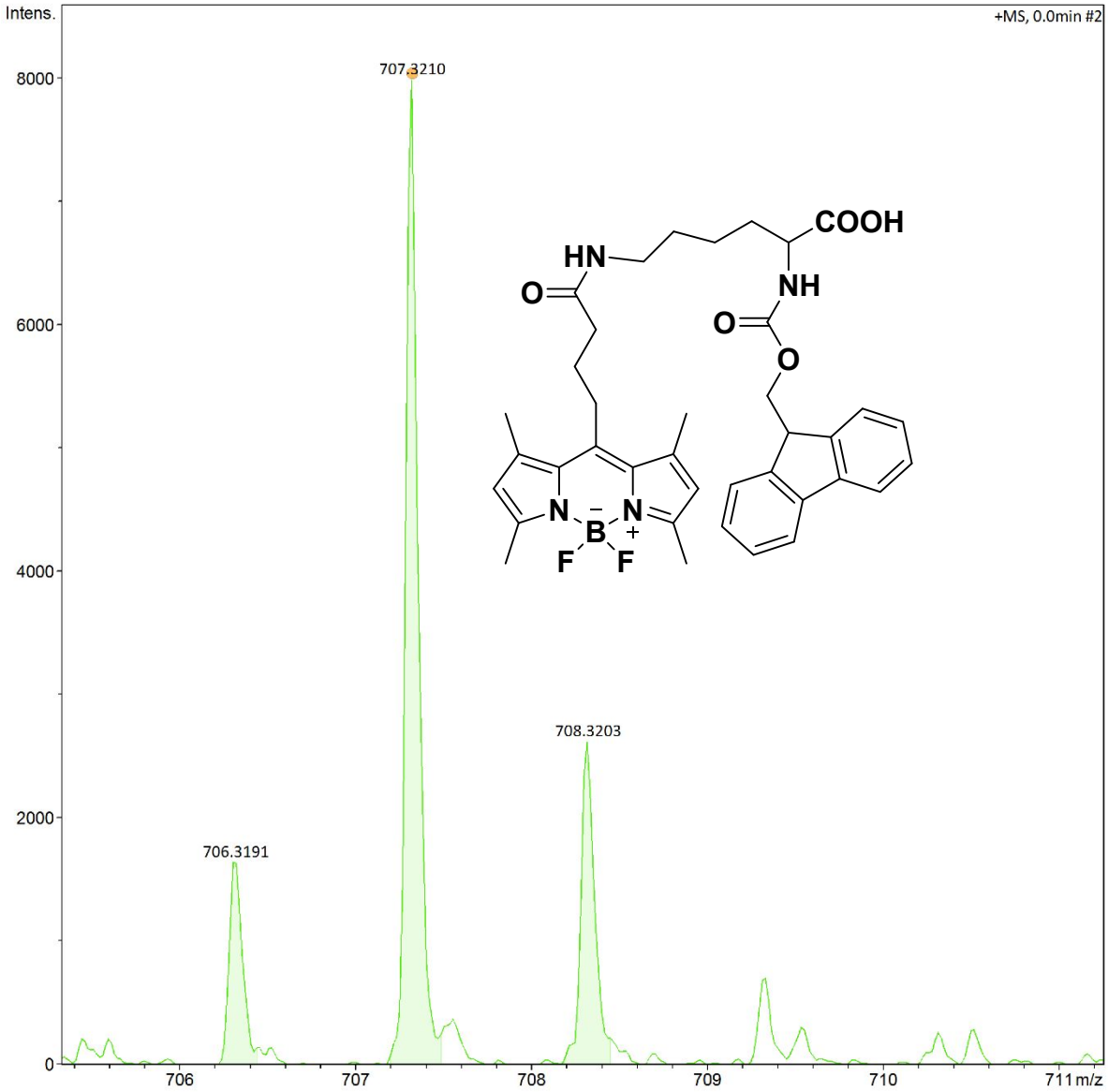

Figure 24: HRMS spectrum for Fmoc-Lys(4-(4,4-Difluoro-1,3,5,7-tetramethyl-4-bora-3a,4a-diaza-s-indacene-8-yl)butyricamide) peptide (**10**) with sodium adduct

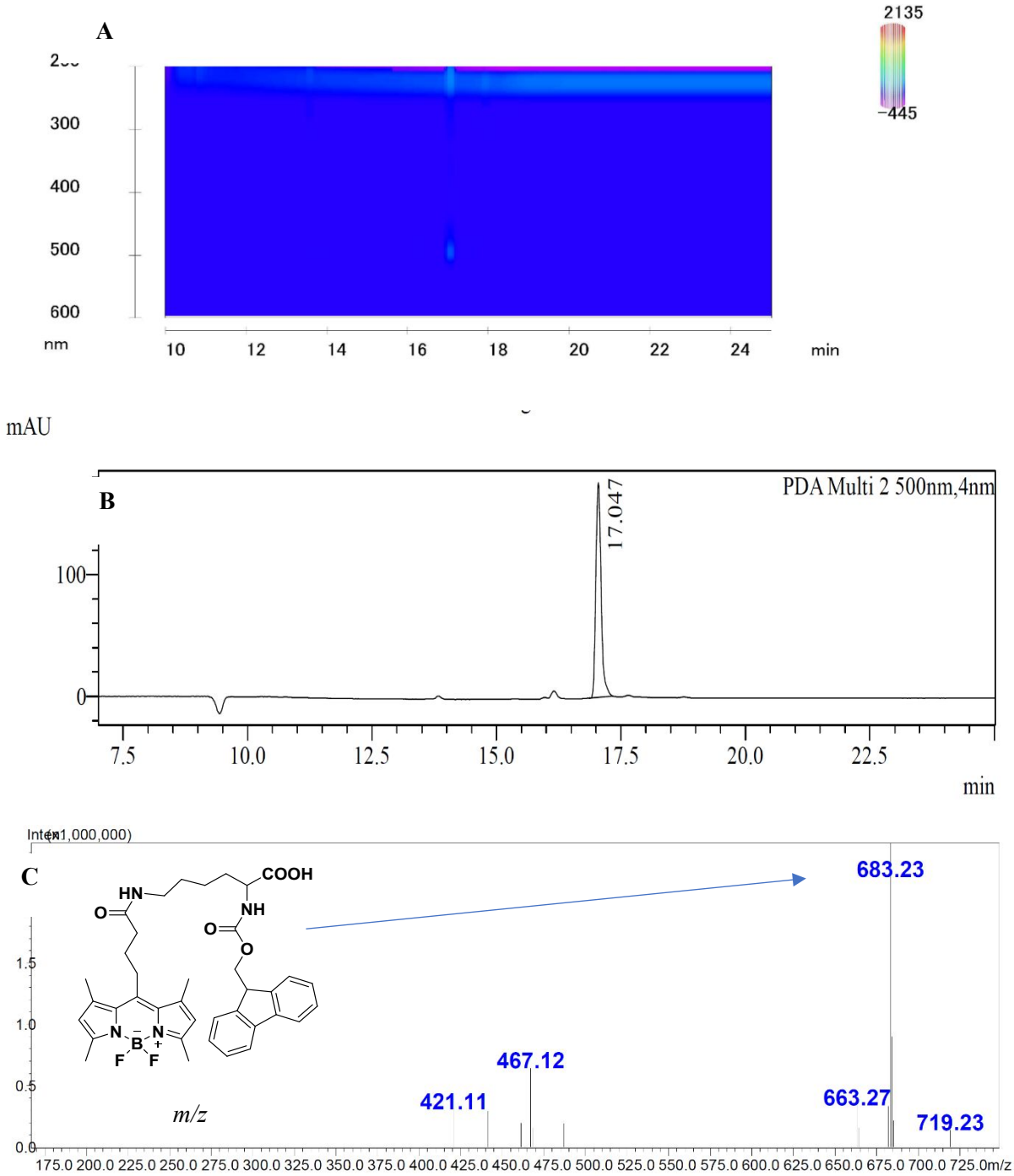

Figure 25: LC-MS-PDA chromatogram of **10. A** PDA showing the purity, **B** LC with retention time and **C** is the MS with the mass in $[M-H]^-$

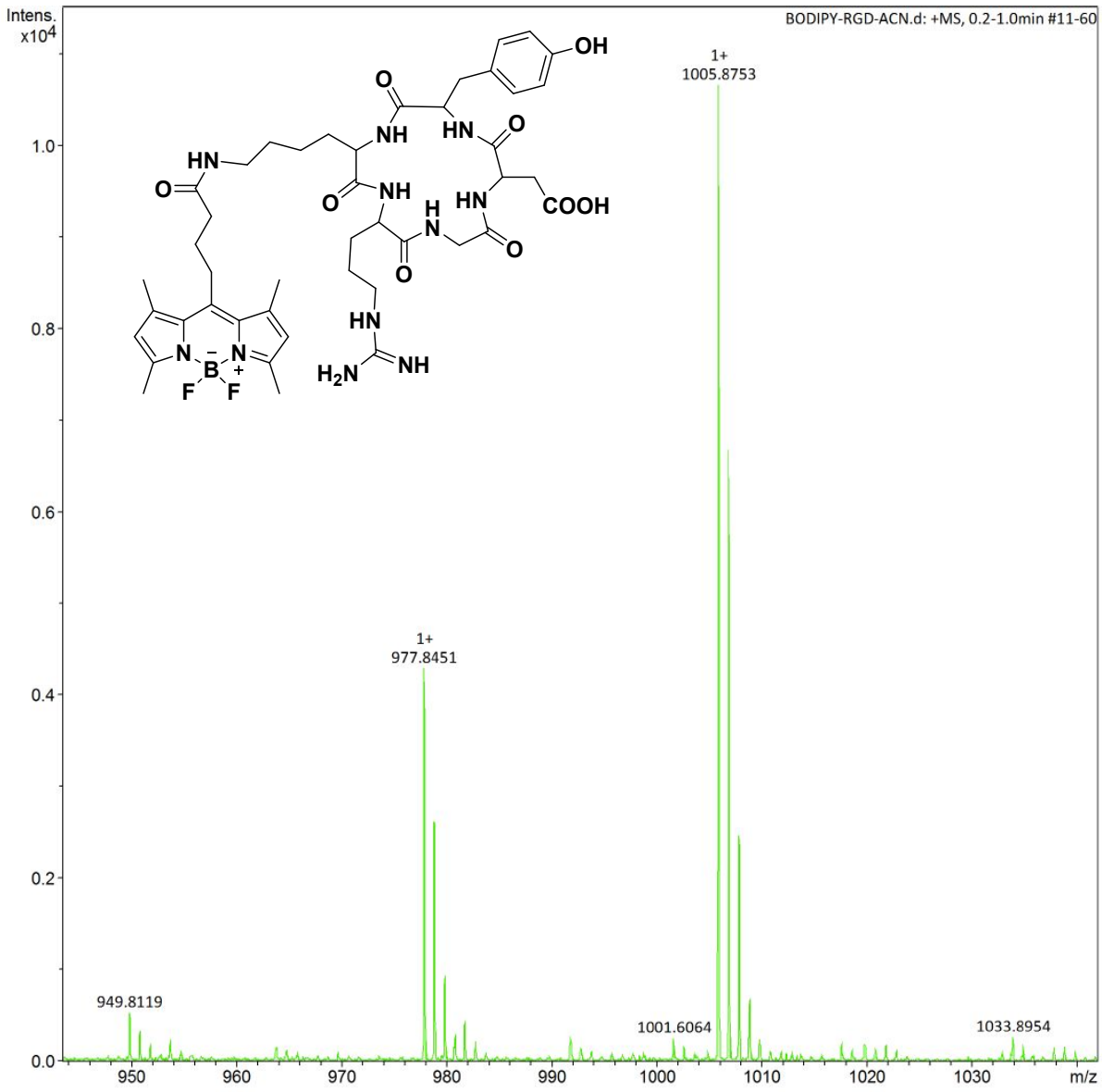

Figure 26: HRMS spectrum for 4-(4,4-Difluoro-1,3,5,7-tetramethyl-4-bora-3a,4a-diaza-s-indacene-8-yl)-butyricamide cyclic RGD peptide (**11**) with acetonitrile adduct

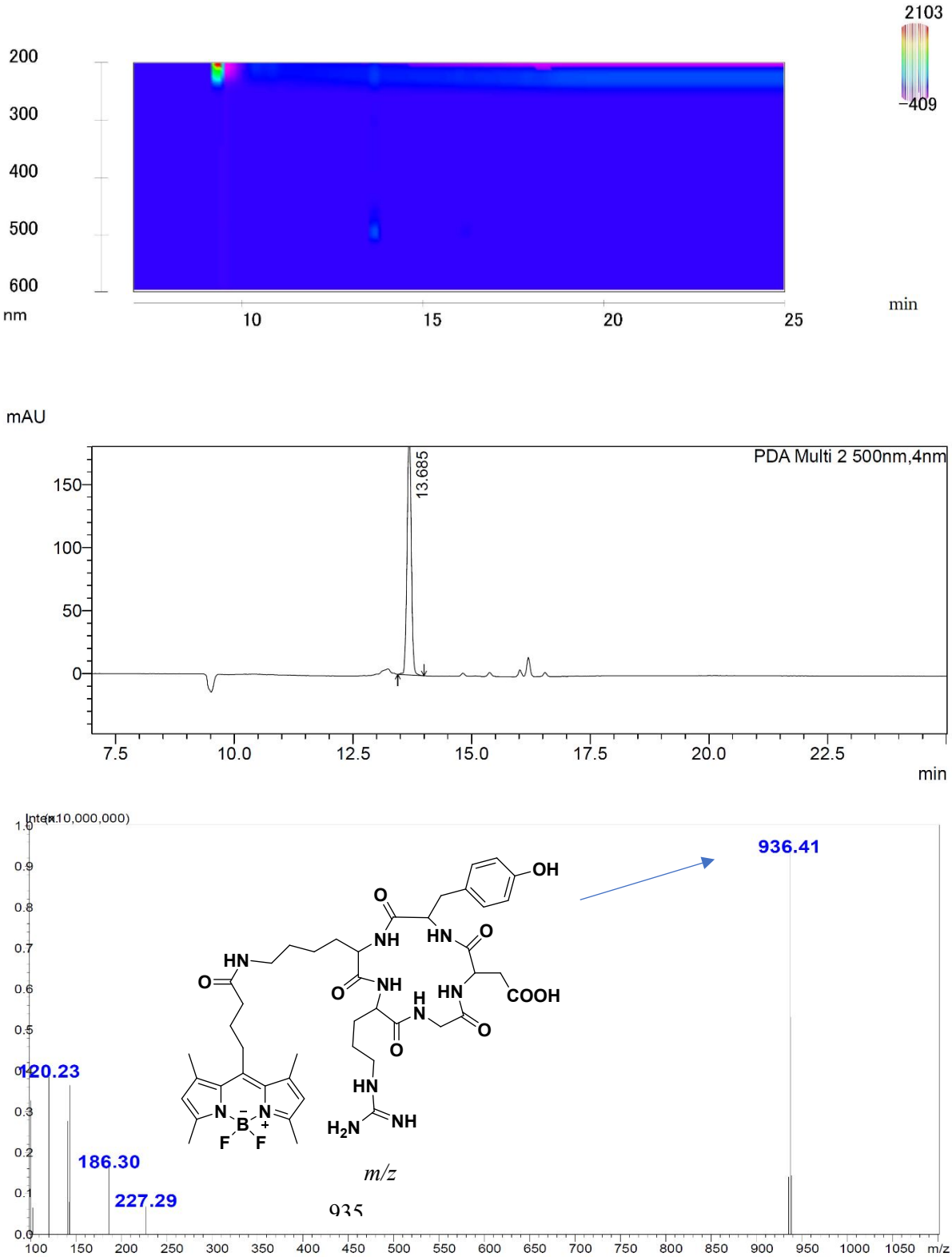

Figure 27: LC-MS-PDA chromatogram of **11. A** PDA showing the purity, **B** LC with retention time and **C** is the MS with the mass in $[M+H]^+$